

Carbon Sequestration in Forests: Current Rates and Attribution

Jim Collatz¹

Chris Williams², Jeff Masek¹

Funding: NASA NNH05ZDA001N-NACP, NASA Carbon Monitoring System



¹NASA Goddard Space Flight Center Biospheric Sciences Laboratory

²Graduate School of Geography, Clark University

US Report to the UNFCCC

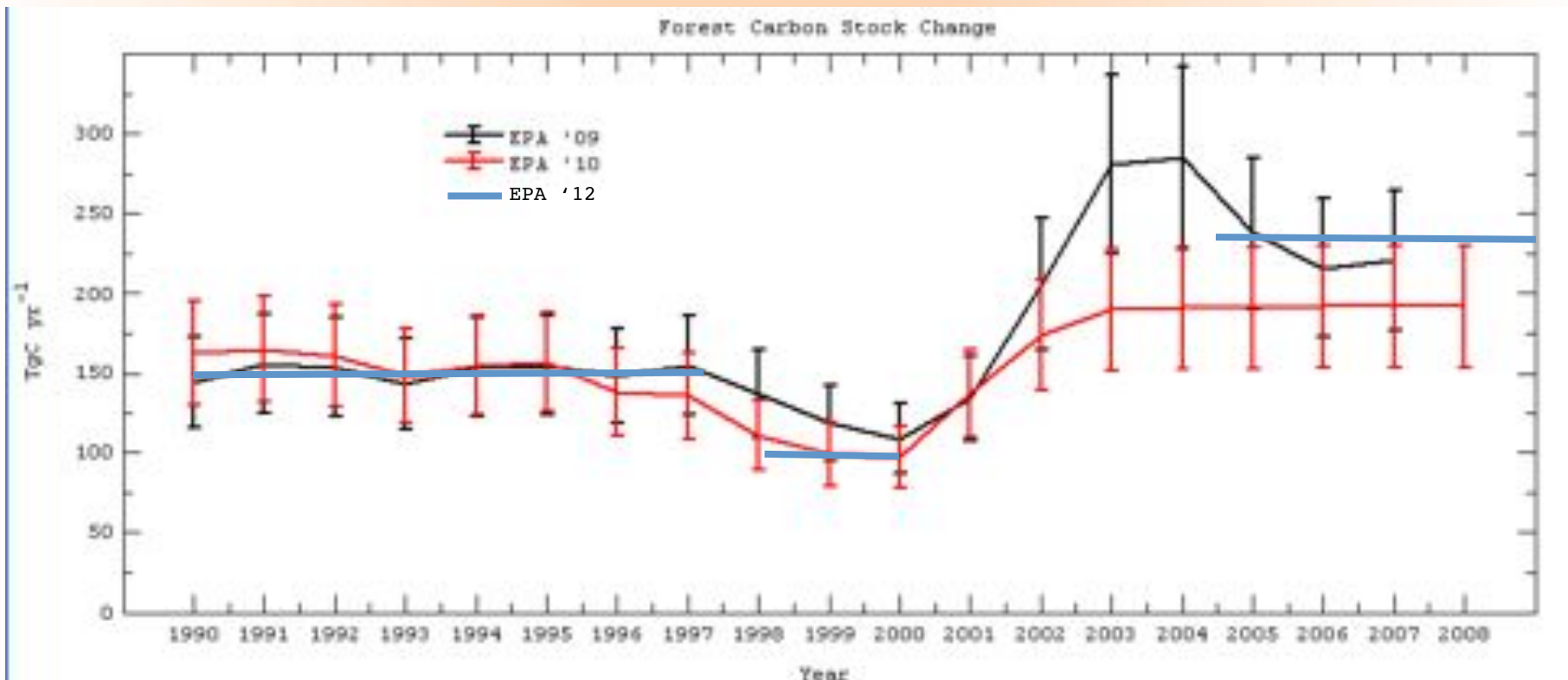
Annual Inventory of Greenhouse Gas Emissions and Sinks

In 2010:

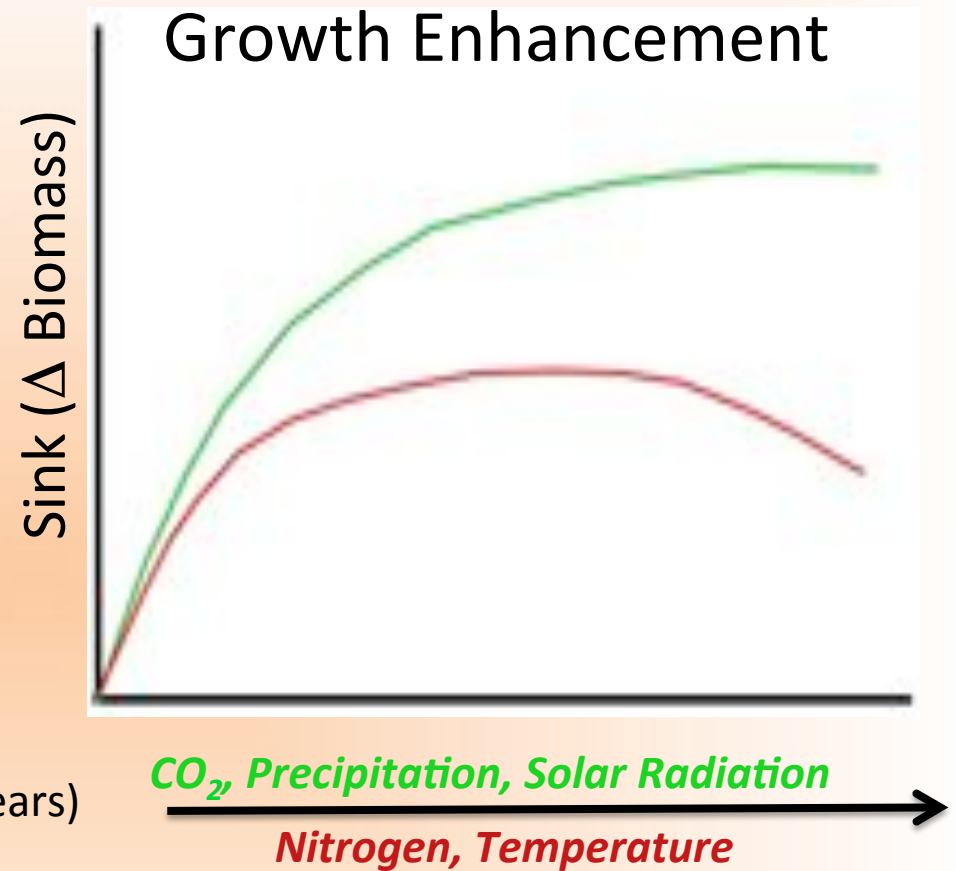
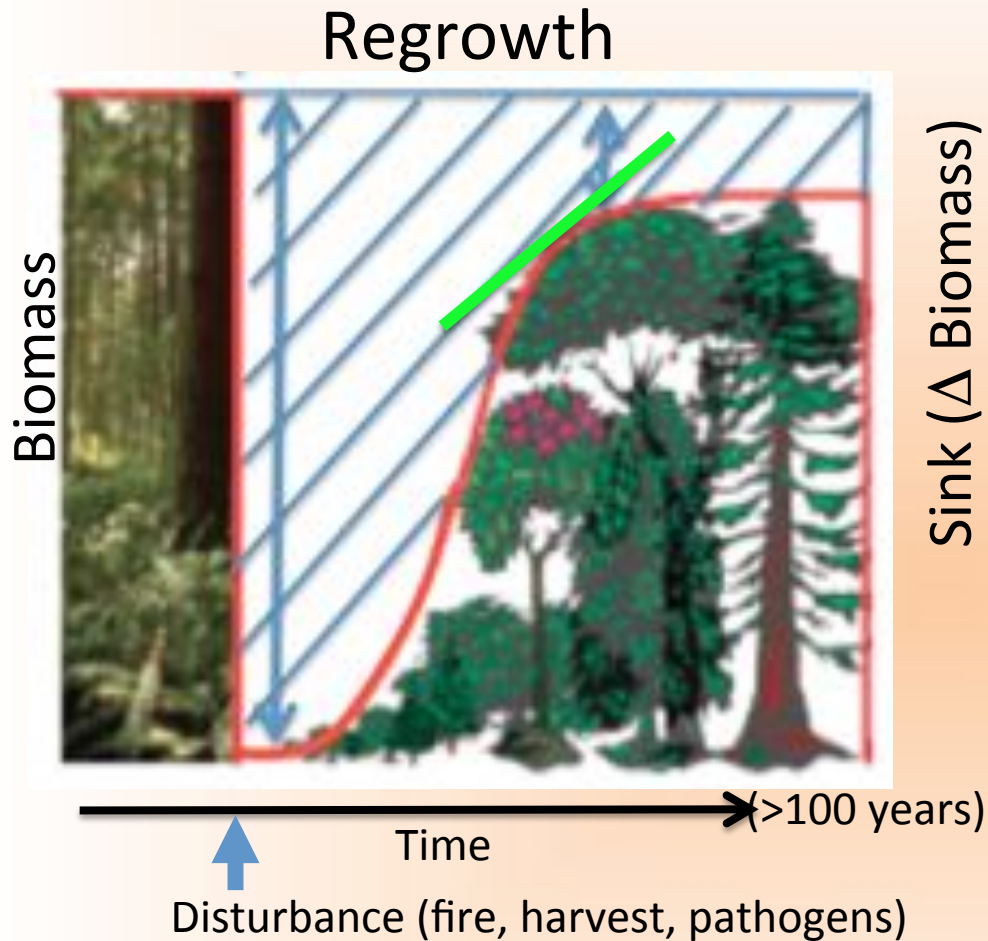
US emissions from fossil fuels: 1,556 Tg C

US forest sink: 251 +/- 80 Tg C or 16% of fossil fuel emissions

Forest sink estimate from FIA (periodic sampling of >150,000 plots) **“The Gold Standard”**



Reasons why a forests would be carbon sinks



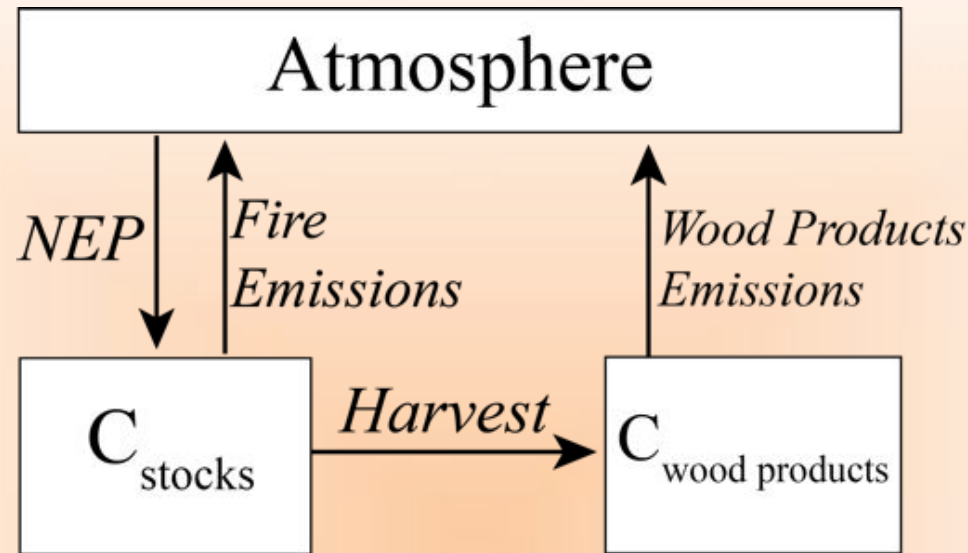
$$NEP = NPP - RH \quad (= GPP - RE)$$

***Regrowth sink: reduced carbon pools

Enhancement: increasing NPP

Other processes less understood: decreases in mortality, respiration attenuation

Forest Sector Carbon Exchanges



Translate ΔC_{stocks} into NEP to diagnose regrowth vs enhancement

$$NEP_{stock\ change} = \Delta C_{stocks} + Harvest + Fire\ Emissions$$

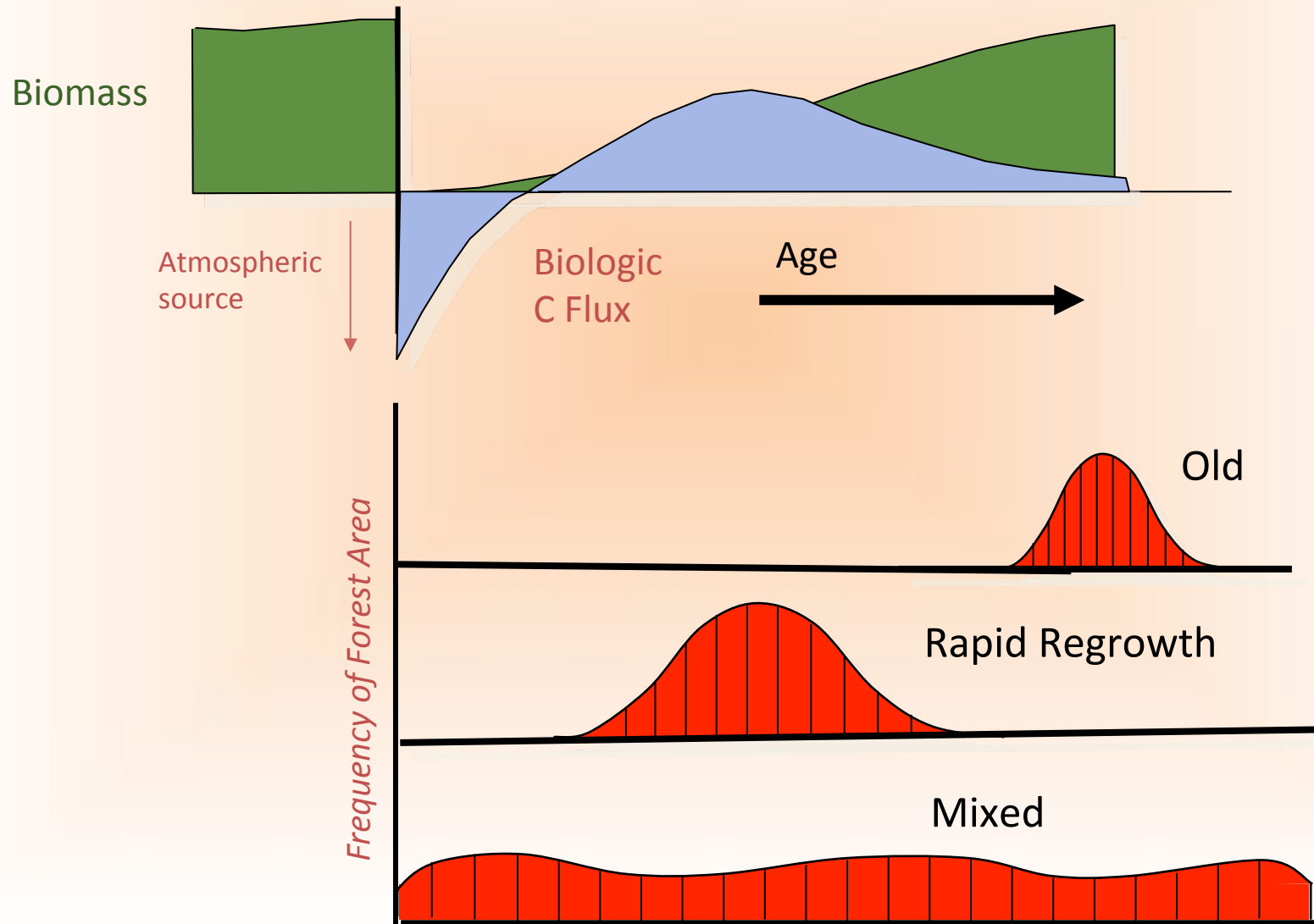
Includes all effects including age and enhancement

$$NEP_{regrowth} = NPP - RH$$

Model accounts for age only (same as Canadian approach for UNFCCC Reporting)

Our Approach:

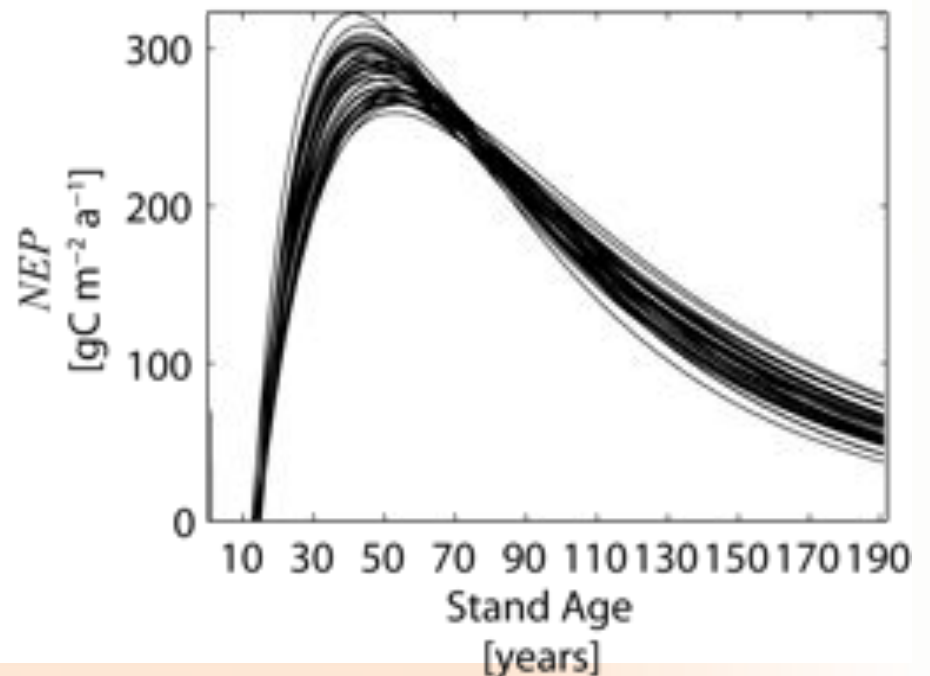
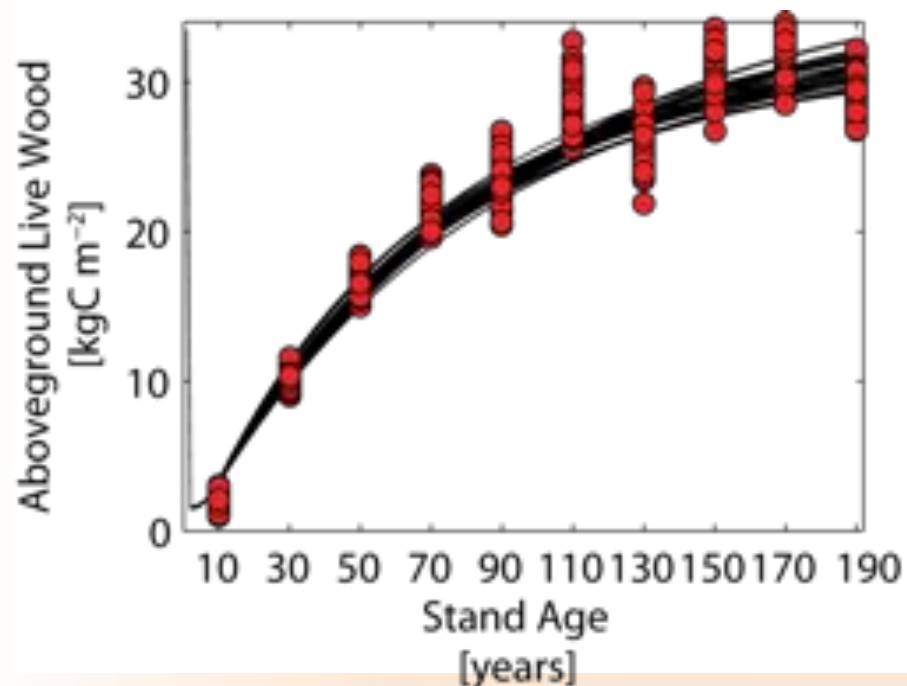
- Calibrate CASA with FIA Forest Age-Biomass data specific to forest type, productivity level and region
- Develop a spatially explicit map of forest age for CONUS (from FIA and Landsat based VCT, Goward et al)
- Assign carbon fluxes based on age of forest





Flux Trajectories

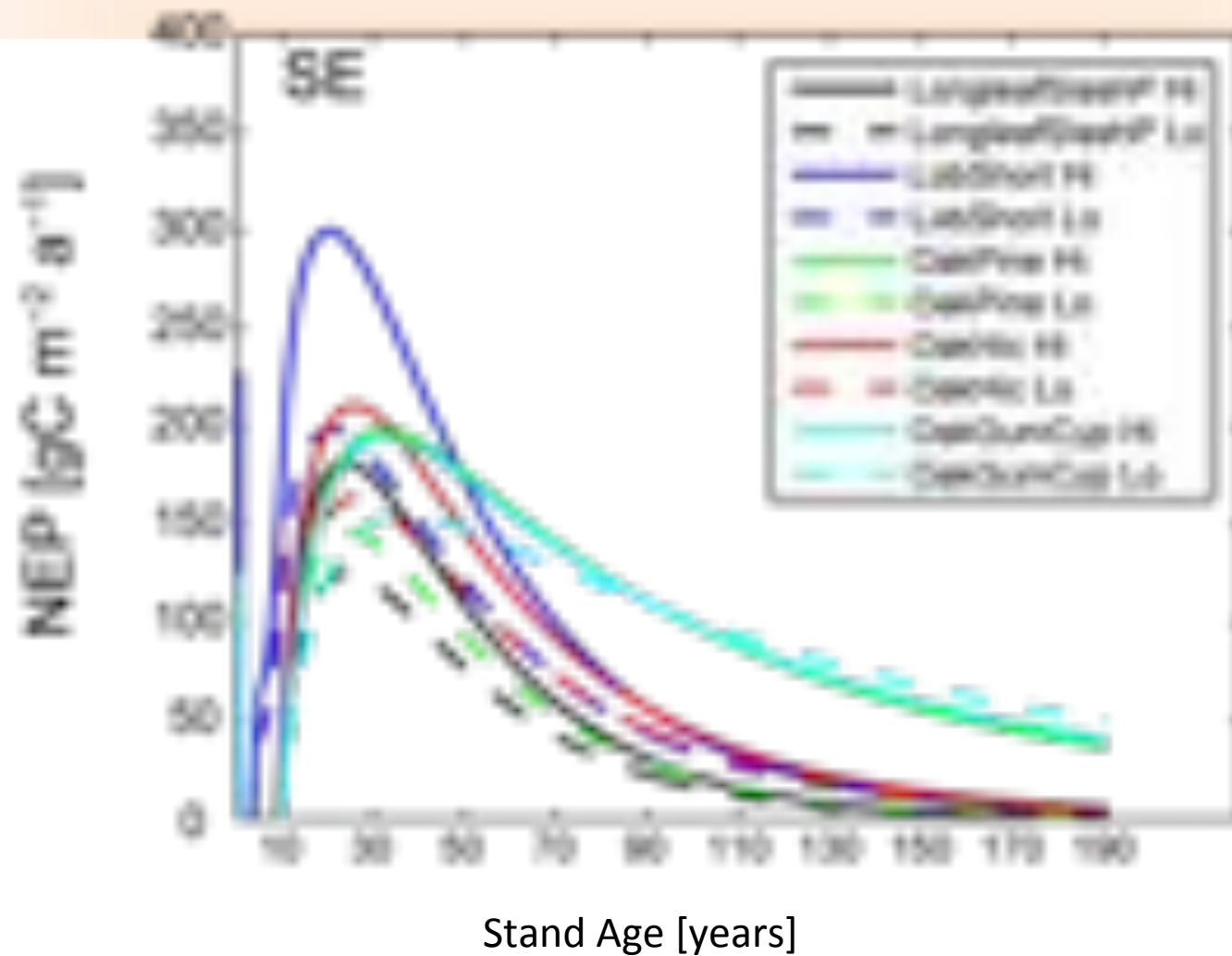
Unique trajectories for regional forest types, productivity classes, and climate settings



Uncertainty formally analyzed with Monte Carlo fitting
biomass sampling error from FIA (+/- 10 to 100%)
volume to carbon conversion (+/- 7%)



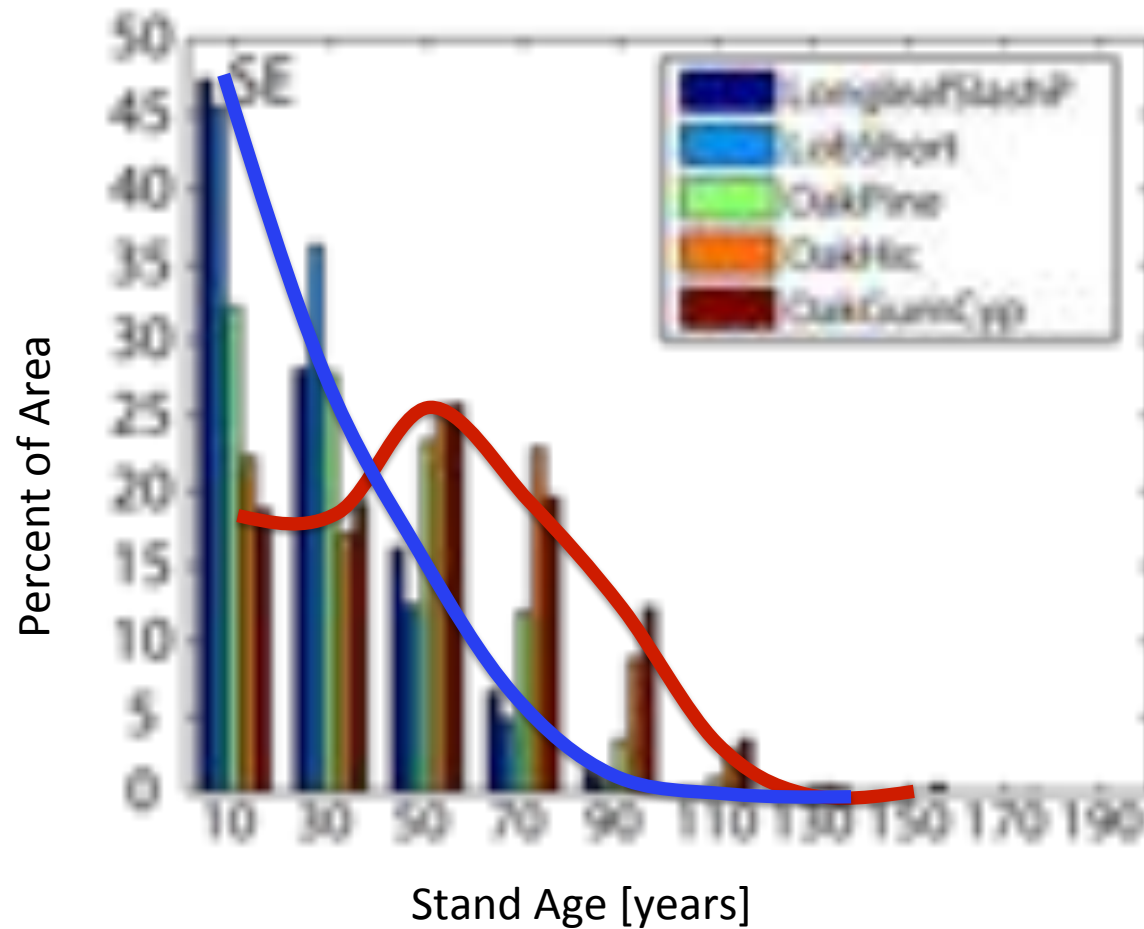
Flux Trajectories Within Regions



Williams et al. (2012) *Glob Biogeochem Cyc*

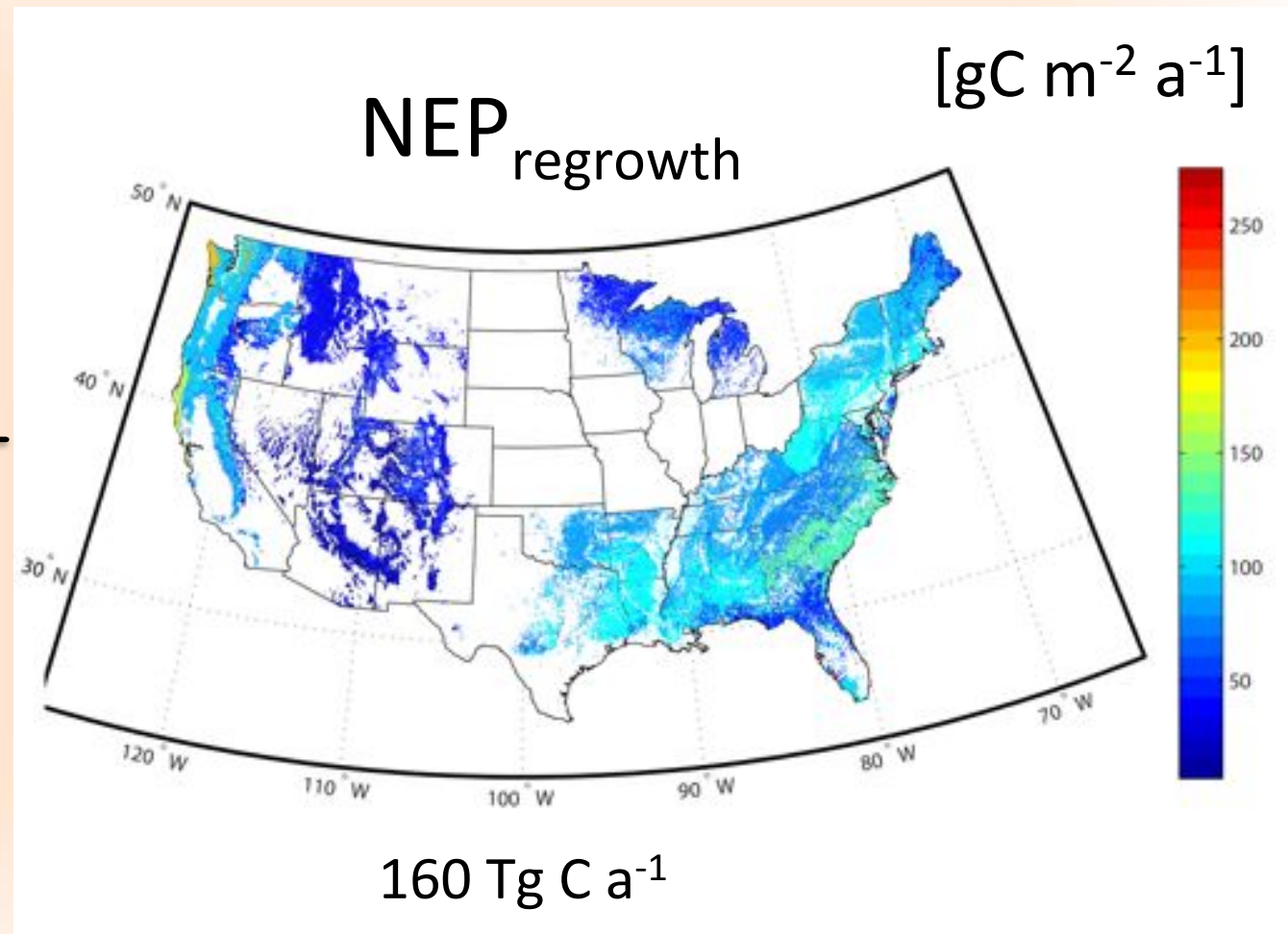
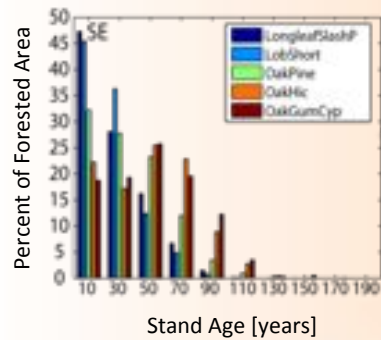
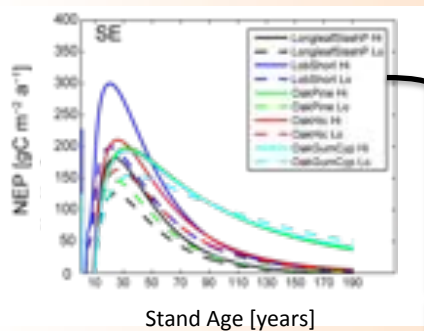


Age Structures Within Regions

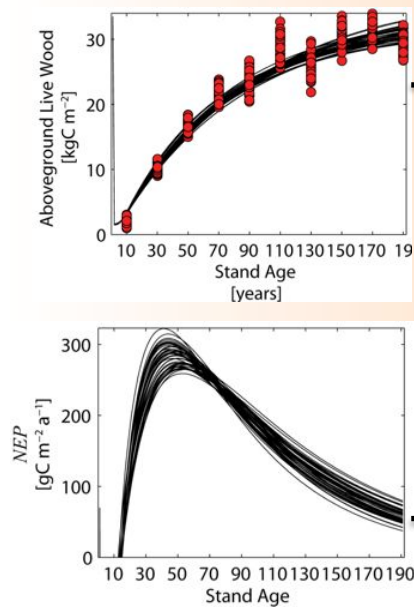




Regrowth Uptake

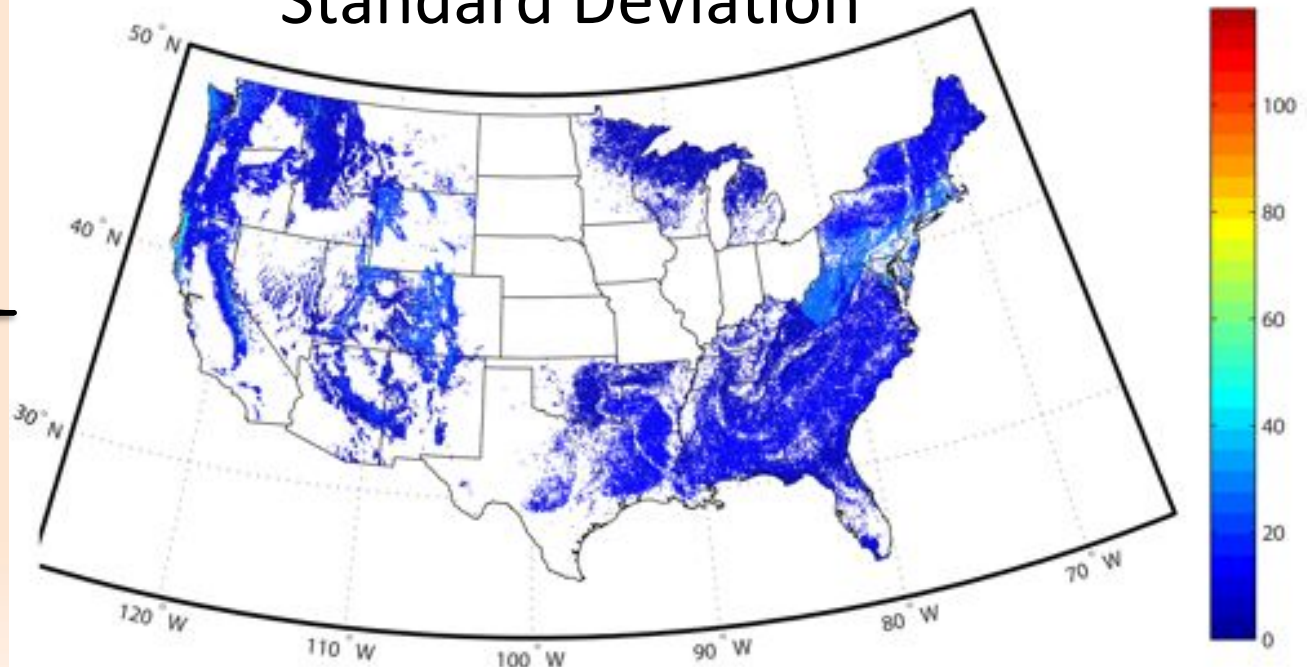


Regrowth Uptake Uncertainty



NEP regrowth modeling Standard Deviation

[gC m⁻² a⁻¹]



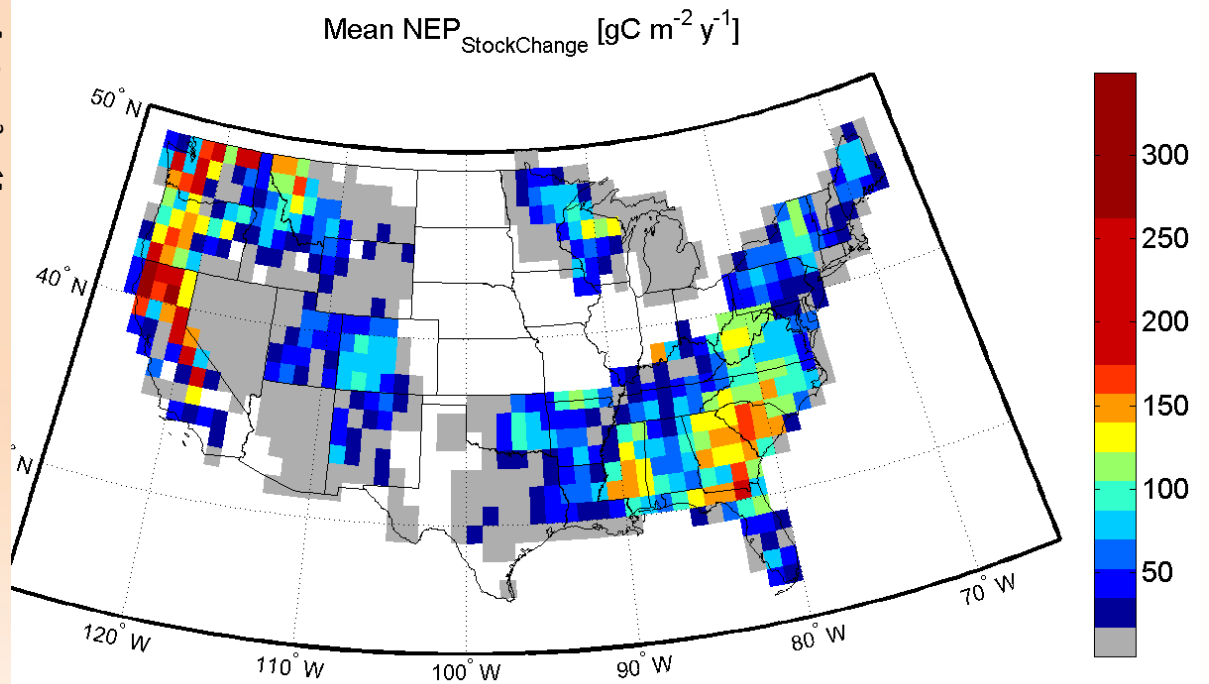
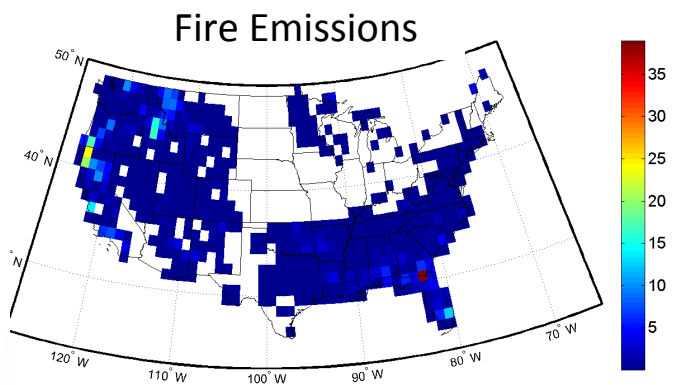
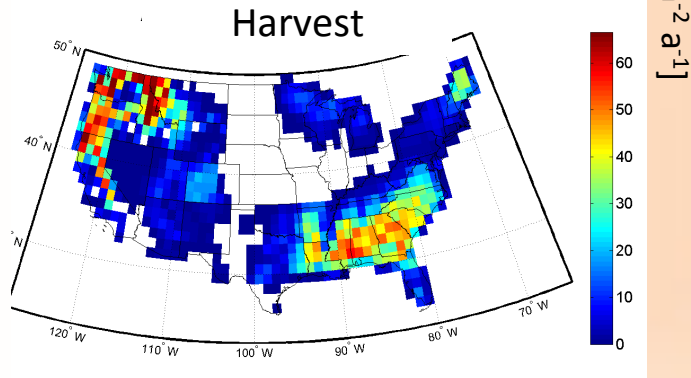
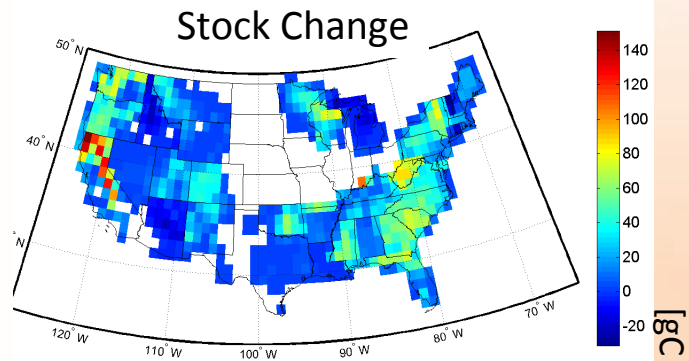
30 Tg C a⁻¹ or 20%



NEP from Stock Changes

$NEP_{\text{stock change}}$

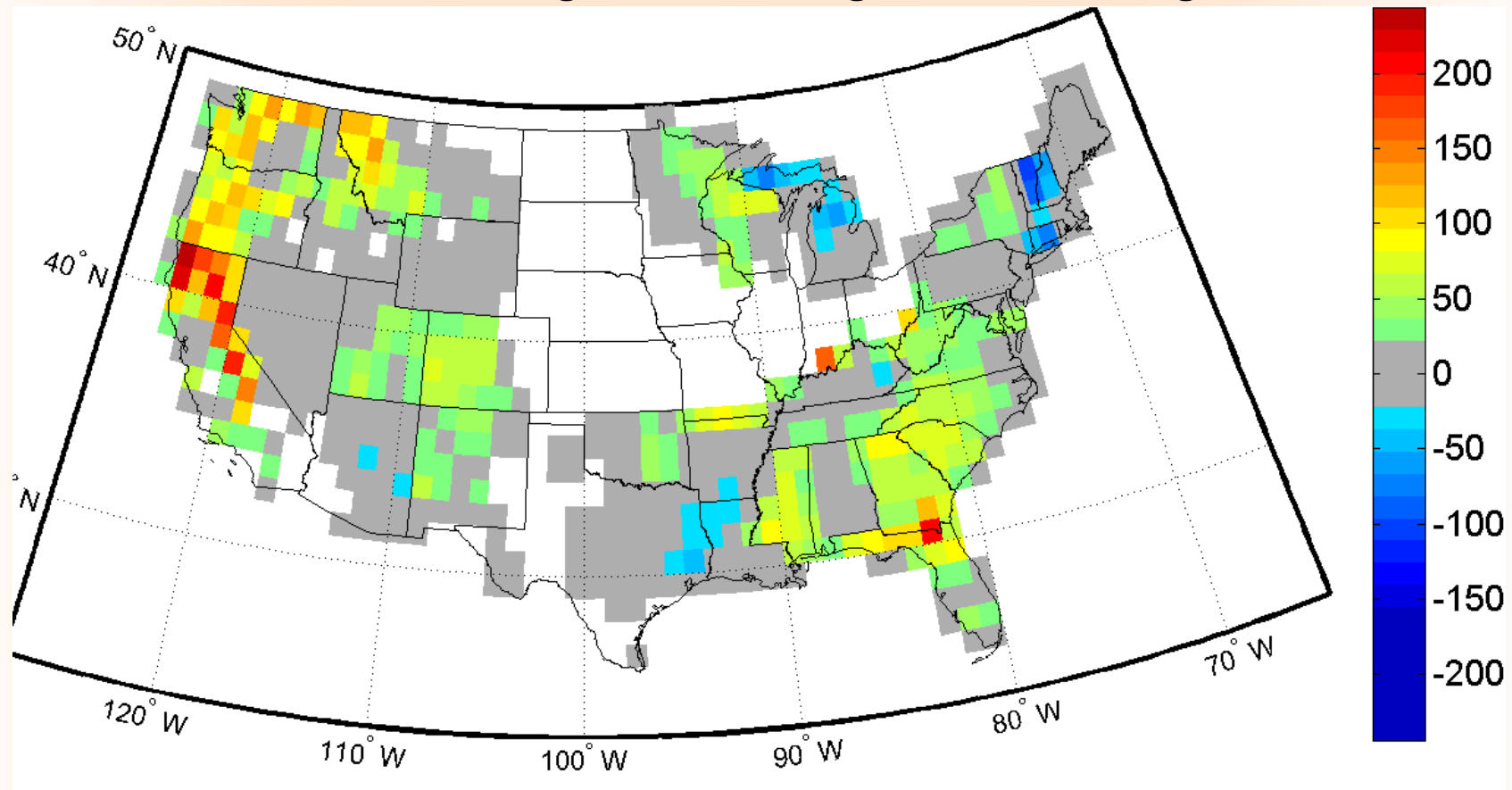
$$NEP_{\text{stock change}} = \Delta\text{Forest Stock} + \text{Harvest Flux} + \text{Fire Flux}$$



310 Tg C a⁻¹

Why are they so different?

$NEP_{\text{stock change}} - NEP_{\text{regrowth modeling}}$

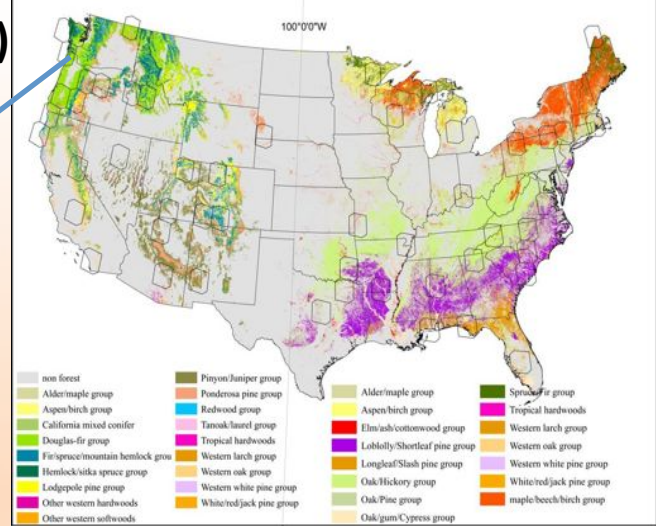


$$310 - 160 = 150 \text{ Tg C a}^{-1}$$

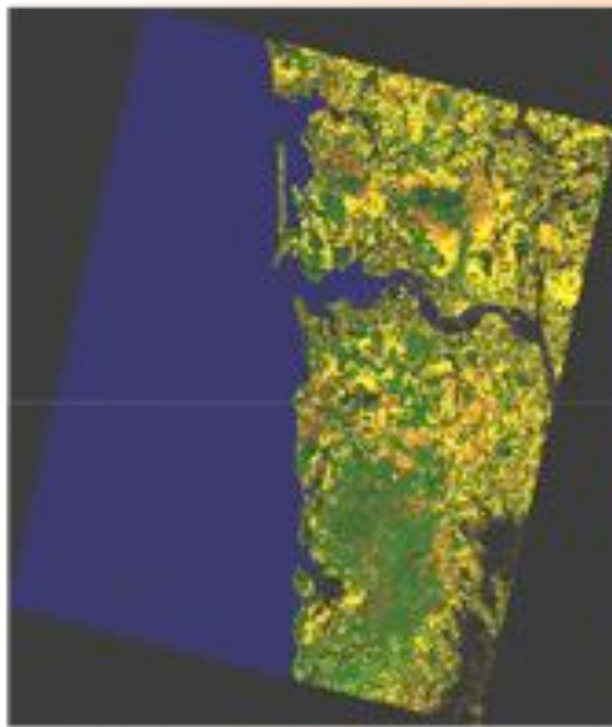
[gC m⁻² a⁻¹]

Stock Change NEP is 2 X larger than Regrowth sink

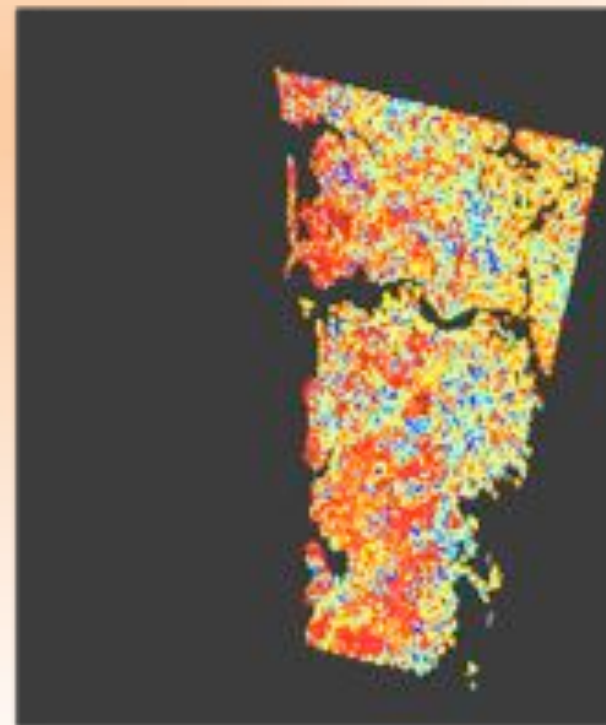
What does the Landsat VCT disturbance history (Goward et al.) tell us about forest age and regrowth?



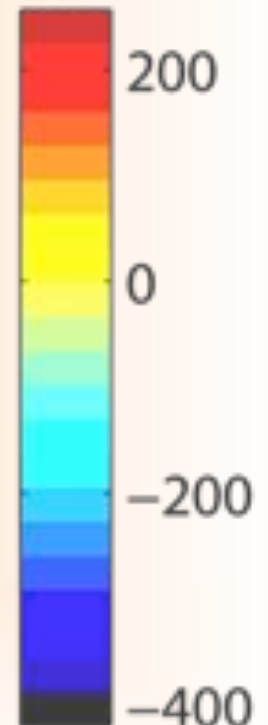
Year of Disturbance



Forest NEP [$\text{gC m}^{-2} \text{a}^{-1}$]



sinks +



sources -

- generate detailed maps of forest NEP, Biomass, etc.

Age Structure of Forests Estimated Using Landsat VCT 1985-2005, FIA < 1985

Introducing fine scale disturbance data reduced the estimated CONUS NEP

Higher disturbance rates especially in regions with large forest industry produce younger forests with lower NEP

***Makes the discrepancy between Stock Change NEP and Regrowth NEP larger
Stock Change NEP 2.6 X larger than Regrowth NEP**

| Region | AREA (1e9m ²) | NEP RS (TgC/yr) | SE (TgC/yr) | NEP FIA (TgC/yr) | SE (TgC/yr) | NPP RS (TgC/yr) | NPP FIA (TgC/yr) | Wood RS (TgC) | Wood FIA (TgC) | <25yr RS % | <25yr FIA % | <5yr RS % | <5yr FIA % | |
|--------|------------------------------|--------------------|----------------|---------------------|----------------|--------------------|---------------------|------------------|-------------------|---------------|----------------|--------------|---------------|------|
| NLS | 212 | 10 | 1.29 | 12 | 1.29 | 85 | 88 | 706 | 851 | 23 | 16 | 4 | 3 | 0.95 |
| NPS | 0 | 0 | 0 | 0 | 0 | 0 | 0 | 0 | 0 | 0 | 0 | 0 | 0 | 0 |
| SE | 355 | 22 | 3.47 | 30 | 3.47 | 308 | 317 | 1700 | 1939 | 51 | 39 | 12 | 8 | 2.27 |
| SC | 420 | 28 | 4.27 | 40 | 4.27 | 316 | 347 | 1948 | 2300 | 45 | 37 | 10 | 8 | 1.96 |
| RMN | 192 | 4 | 1.81 | 7 | 1.81 | 65 | 73 | 762 | 914 | 34 | 21 | 8 | 5 | 1.55 |
| RMS | 493 | 10 | 5.51 | 11 | 5.51 | 87 | 88 | 1265 | 1372 | 26 | 1 | 7 | 0 | 1.2 |
| PSW | 127 | 8 | 2.81 | 13 | 2.81 | 89 | 97 | 834 | 1236 | 28 | 11 | 9 | 2 | 1.29 |
| PNW | 202 | 10 | 2.93 | 18 | 2.93 | 167 | 171 | 1483 | 1788 | 45 | 19 | 8 | 4 | 1.9 |
| Total | 2339 | 120 | 27.88 | 164 | 27.88 | 1377 | 1451 | 11094 | 13015 | 30 | 17 | 7 | 4 | 1.34 |

East

1.46721854
53

West

1.416992
11

Sensitivity Analyses

Errors in the representation of biomass accumulation with stand age could cause large errors in estimated fluxes

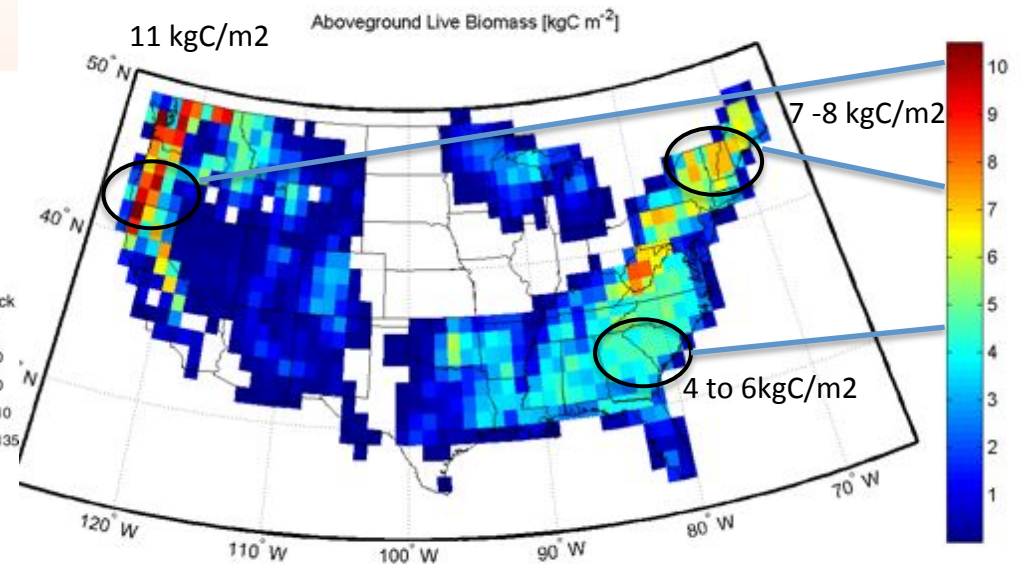
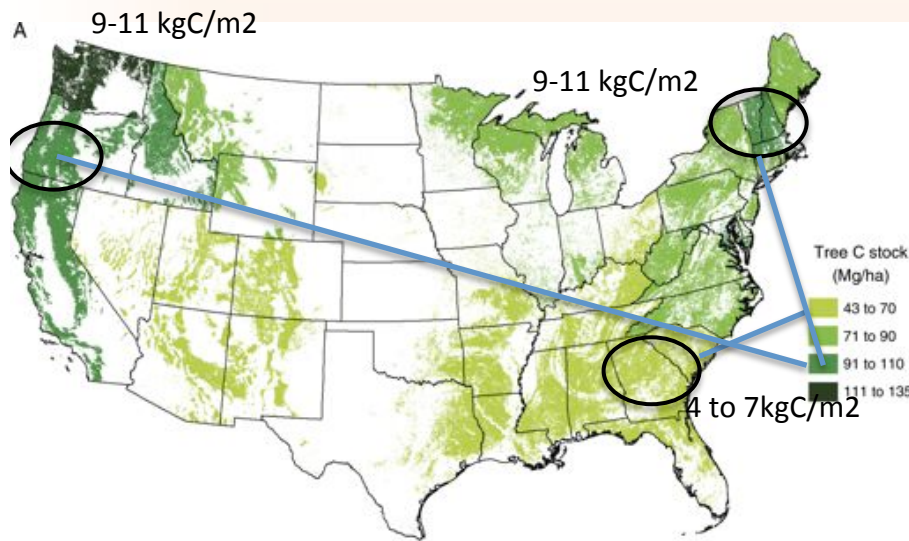
- 1) wood turnover has a large influence on rate of biomass increase and is poorly constrained
- 2) stand thinning (selective logging) may lower biomass in the inventory without resetting age

3) age reporting may be biased

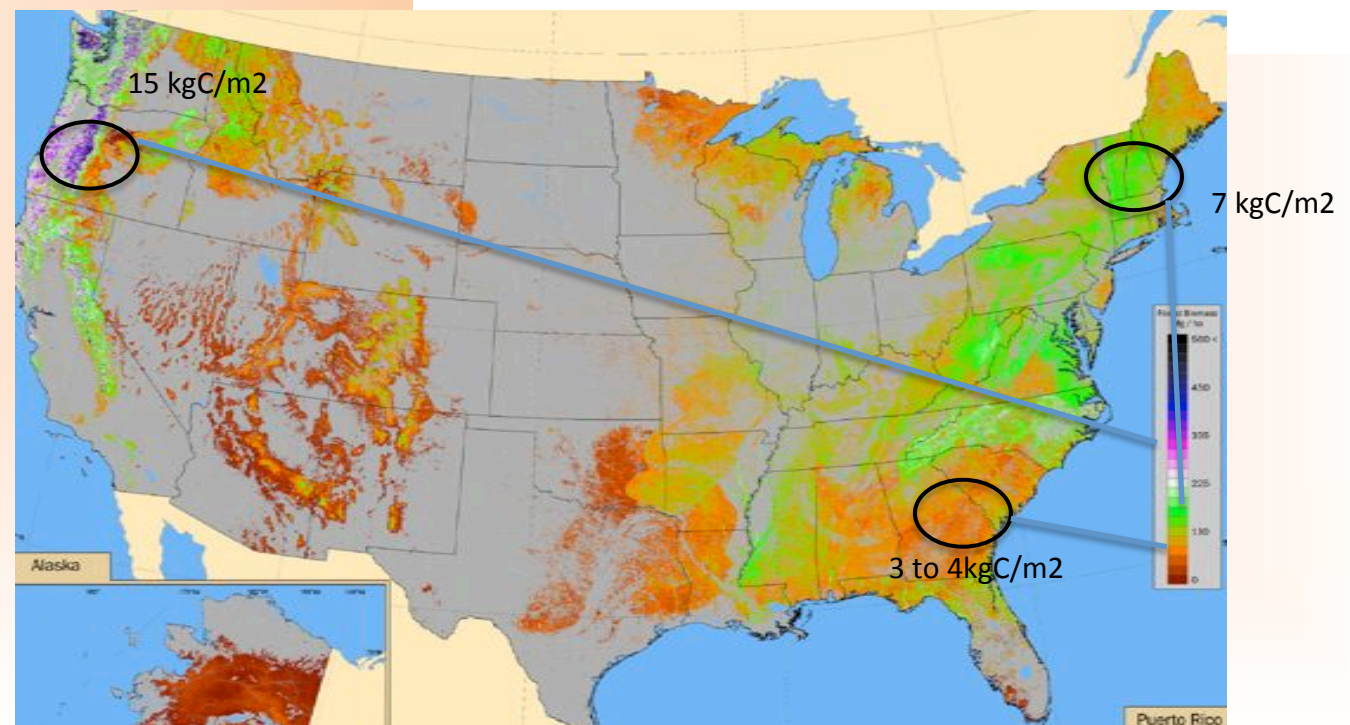
| | <i>NEP</i> [Tg C a ⁻¹] | <i>NPP</i> [Tg C a ⁻¹] | <i>AGB</i> [Pg C] |
|-----------------------------|---------------------------------------|---------------------------------------|----------------------|
| Original Results | 164 (28) | 1451 | 13.0 |
| Wood Turnover Increased 10% | 169 (30) | 1714 | 13.2 |
| Biomass Increased 10% | 187 (32) | 1761 | 14.2 |
| Stand Age –5 years | 173 (30) | 1860 | 13.7 |
| Stand Age +5 years | 162 (33) | 1401 | 12.3 |

Biomass would have to be 70% higher to produce the $NEP_{stock\ change}$

McKinley et al '11 from Woodbury



Blackard et al '08
Above ground dry
weight biomass



Recent Studies presenting Evidence of Growth Enhancement

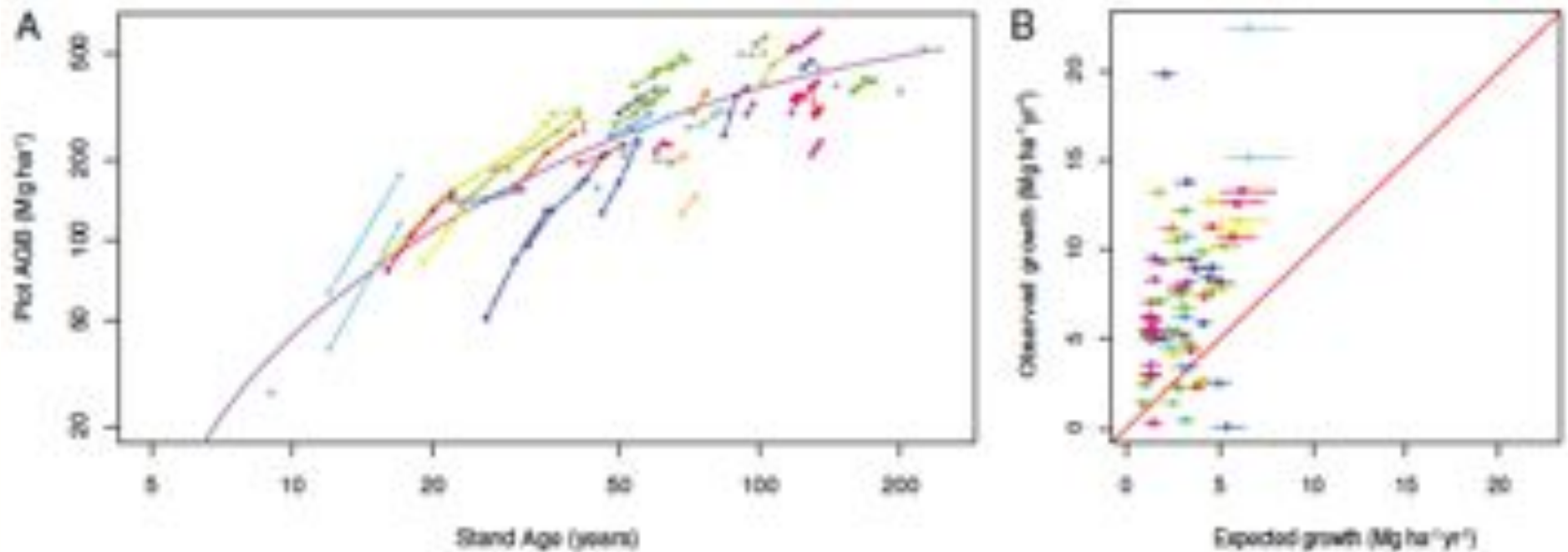
Methods Employed: Inventory, Modeling, Eddy Covariance, Tree Ring

| Source | Region | <i>NPP</i> | <i>NEP_e</i> | <i>ΔNPP</i> | <i>ΔNPP%</i> | <i>ΔNEP</i> | Approaches † | Factors‡ |
|-----------------------|-------------------|------------|------------------------|--------------|--------------|--------------|----------------------------------|--|
| Thomas et al. 2010 | US northeast | 650 | 11 | 0.37 | 0.1% | <i>0.09</i> | ΔAGB, 1 | N |
| Houghton et al. 2003 | Global land | 400 | 13 | <i>0.43</i> | <i>0.1%</i> | <i>0.11</i> | Budget, 1 | all |
| Bellassen et al. 2011 | Europe | 604 | <i>30</i> | 1.00 | 0.2% | 0.87 | Model, 1 | CO ₂ , C |
| Beta Factor 50% | -- | 650 | <i>35</i> | 1.16 | 0.2% | <i>0.29</i> | Model, 1 | CO ₂ |
| Zaehle et al. 2006 | Europe | 750 | 33 | <i>1.10</i> | <i>0.3%</i> | <i>0.28</i> | Model+, 1 | CO ₂ , C |
| Pan et al. 2009 | US Mid-Atlantic | 765 | 83 | 2.25 | 0.3% | 0.83 | Model, -- | CO ₂ , C, N, O ₃ |
| Williams et al. 2011 | US | 744 | 81 | <i>2.70</i> | <i>0.6%</i> | <i>0.68</i> | Model+, 1 | all |
| Desai et al. 2007 | US Wisconsin | 402 | 100 | <i>3.30</i> | <i>0.8%</i> | <i>0.83</i> | Model, 1 | CO ₂ , C |
| Cole et al. 2010 | US West | -- | -- | -- | 1.1% | -- | ΔAGB, -- | all |
| McMahon et al. 2010 | Global SERC Plots | 808 | 808 | <i>27.00</i> | <i>3.3%</i> | <i>6.79</i> | ΔAGB, 1 | all |
| Pilegaard et al. 2011 | Denmark | 864 | <i>79</i> | <i>36.00</i> | <i>4.2%</i> | 23.00 | EC, 2 | all |
| Urbanski et al. 2007 | US Massachusetts | 650 | <i>125</i> | <i>30.00</i> | <i>4.6%</i> | 13.00 | EC, 2 | all |
| Dragoni et al. 2010 | US Indiana | 650 | <i>175</i> | <i>32.00</i> | <i>4.9%</i> | 10.00 | EC, 2 | all |
| Average | | 661 | 130 | 11.4 | 1.58% | 4.7 | $\text{gC m}^{-2} \text{y}^{-1}$ | |
| Median | | 650 | 80 | 2.5 | 0.62% | 0.8 | | |



Plots Show Accelerated Growth

Present-day growth rates exceed those expected from chronosequences of biomass regrowth with forest age



McMahon et al (2010) PNAS

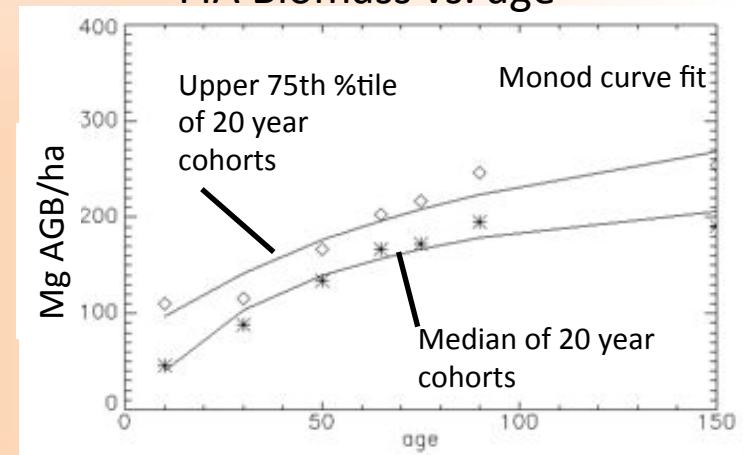
Analysis of individual FIA Plot data for Eastern US Forests (>1000 Plots in Each State)

Construct age dependent biomass trajectories for major forest types (Regrowth)

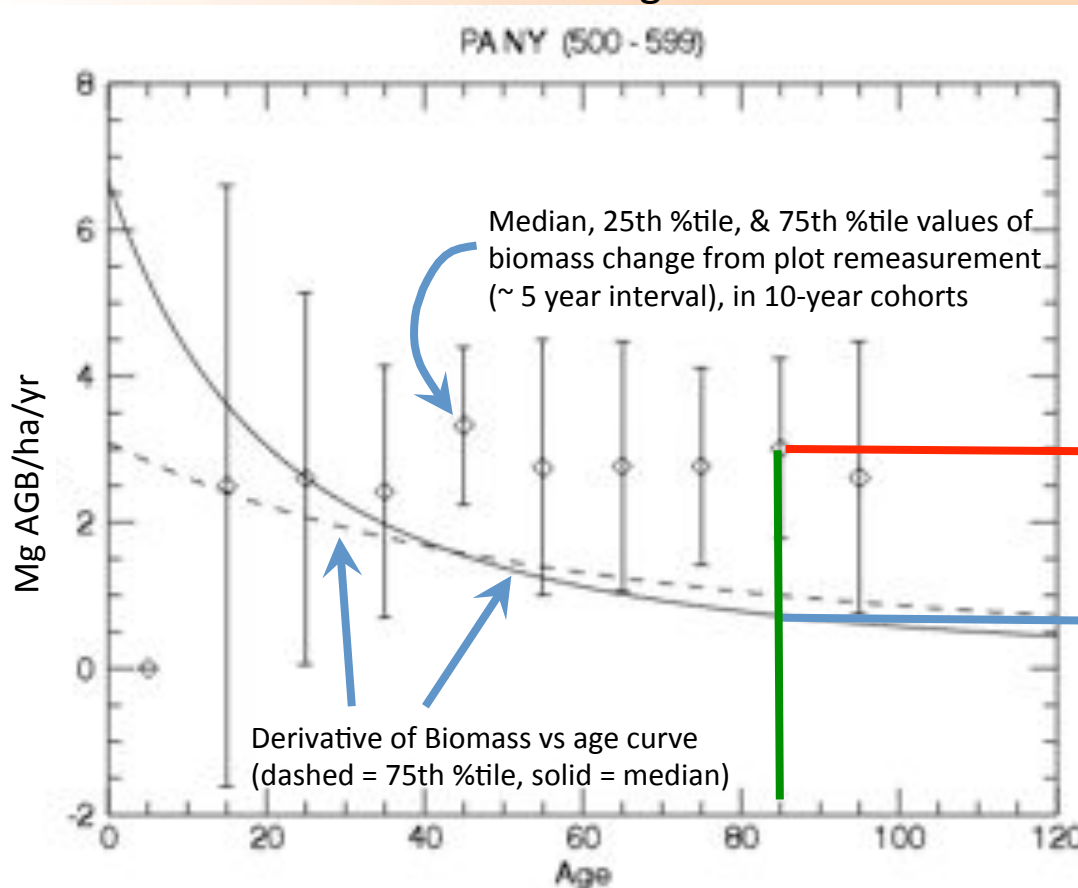
Estimate the change in biomass of individual plots between the 2 most recent inventories (Stock Change)



FIA Biomass vs. age



Biomass change rate



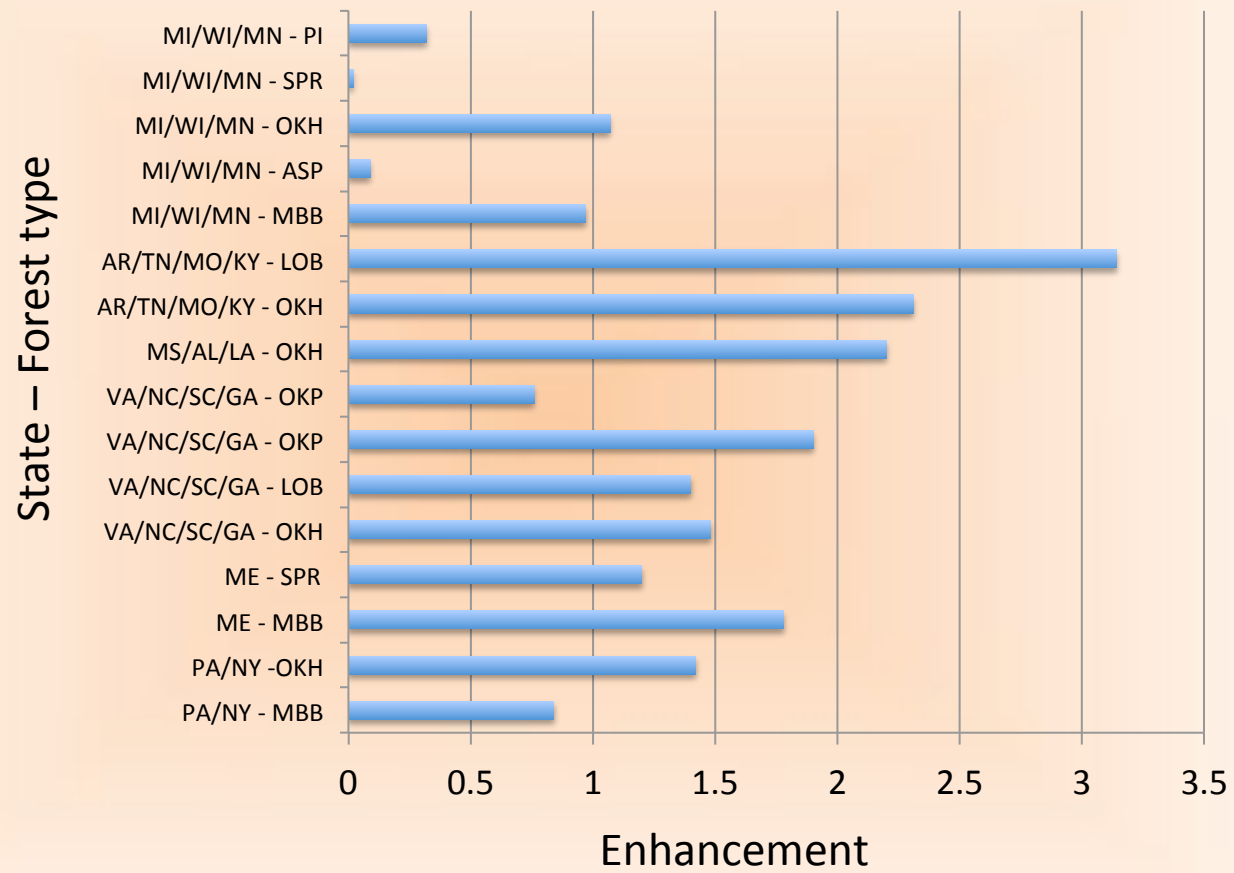
85 year old forests

Stock Change = 3 MgC/ha/yr (300 gC/m²/yr)

Regrowth = 0.7

$$\text{Enhancement} = \frac{3.0 - 0.7}{0.7} = 2$$

Age-weighted Growth Enhancement by FIA Type/Region

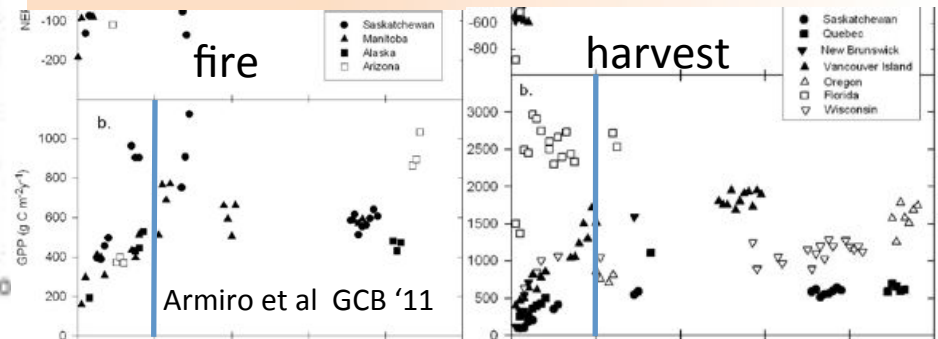
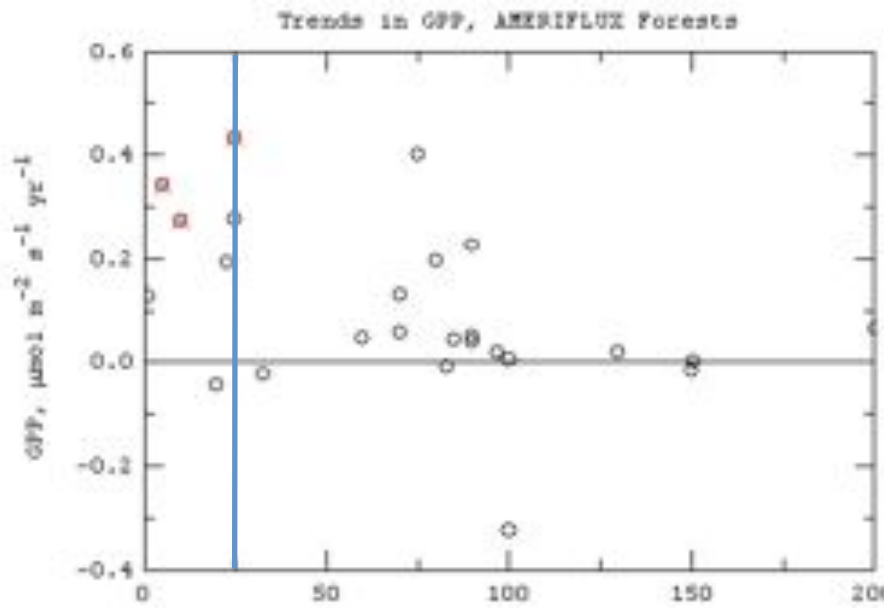


Evidence for Enhancement in Eddy Covariance Measurements

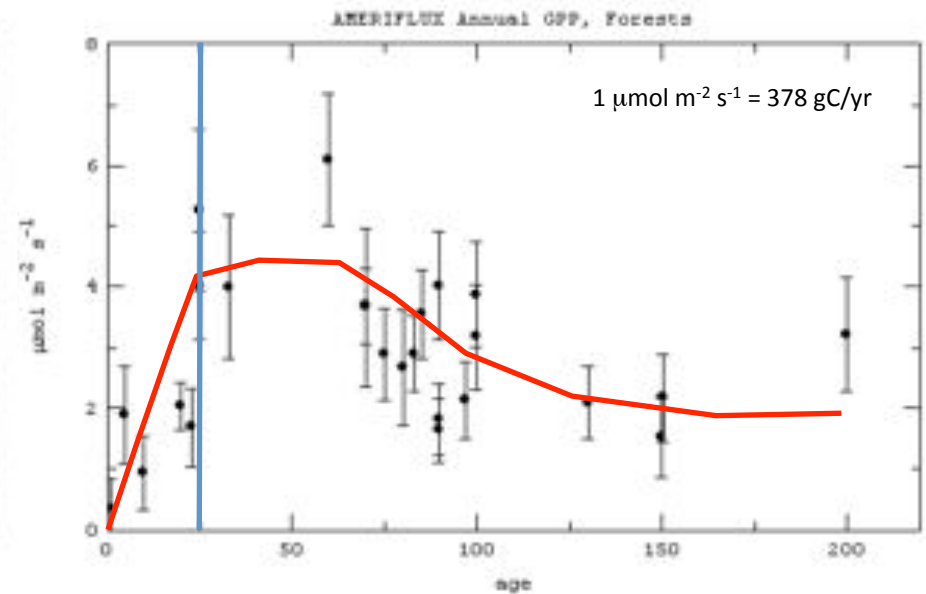
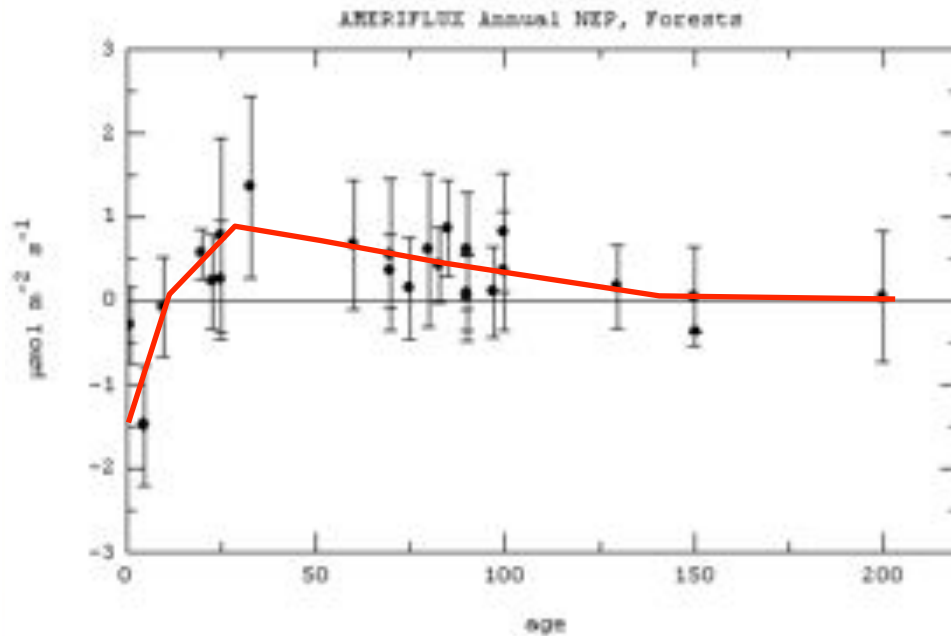
25 forest sites US and Southern Canada.

Most sites show positive trends in GPP

Not expected based understanding of Regrowth dynamics



Armiro et al GCB '11

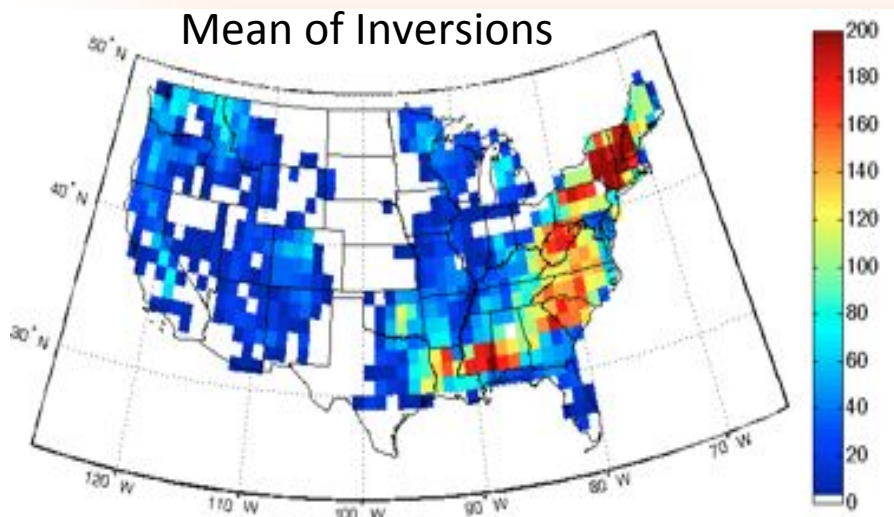


$1 \mu\text{mol m}^{-2} \text{s}^{-1} = 378 \text{ gC/yr}$

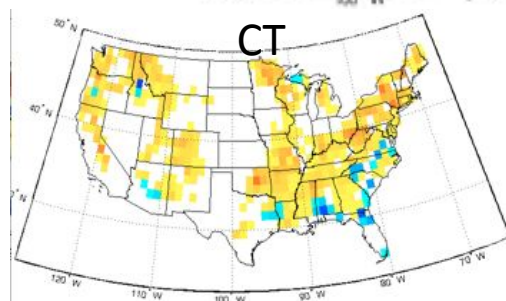
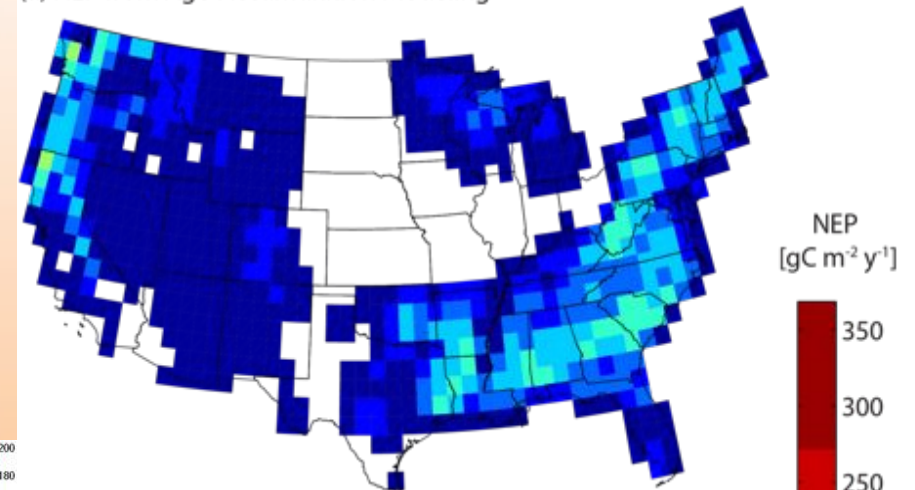
Data courtesy of K. Schaefer

Inversions can't yet reconcile magnitude and distribution of Forest Sinks

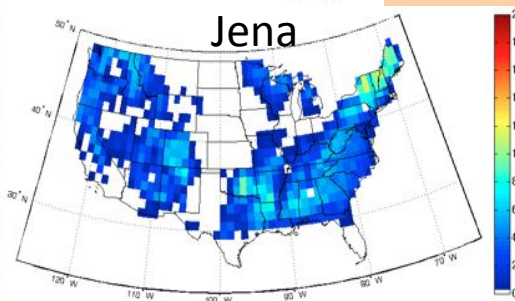
Mean of Inversions



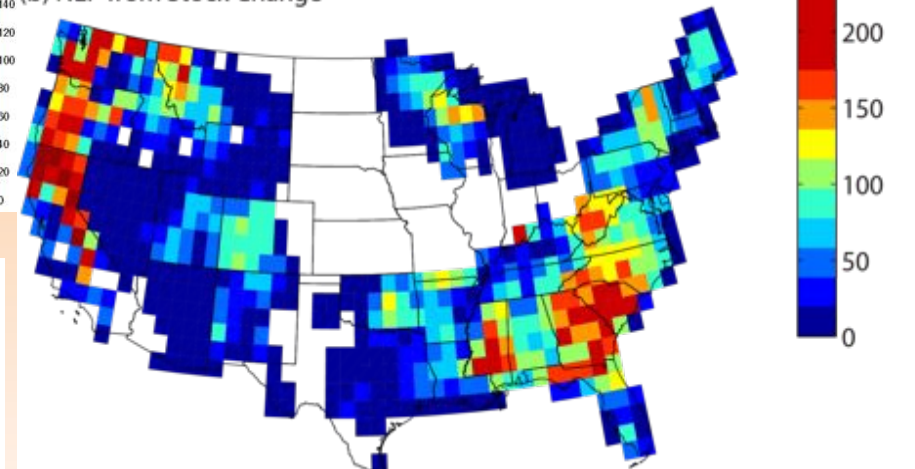
(a) NEP from Age-Accumulation Modeling



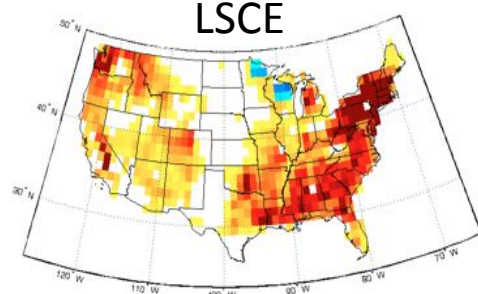
Jena



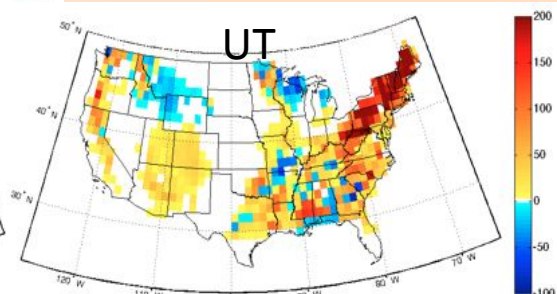
(b) NEP from Stock Change



LSCE



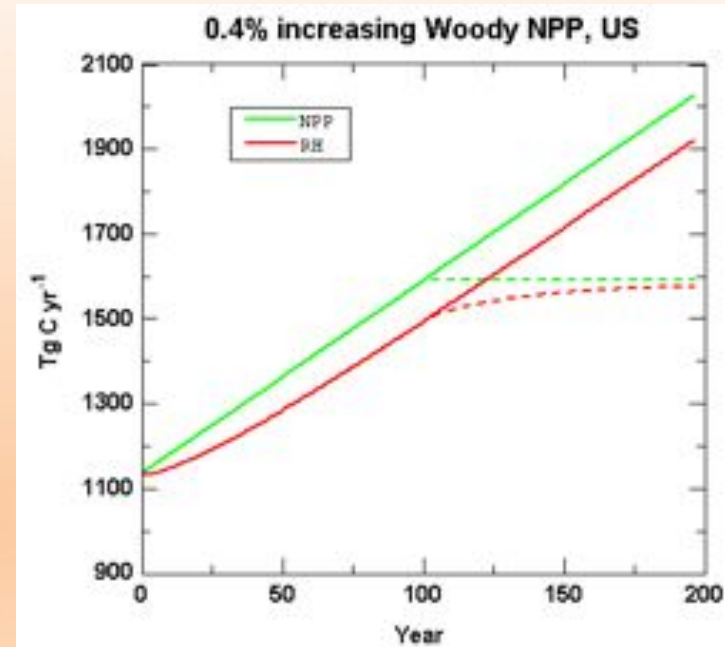
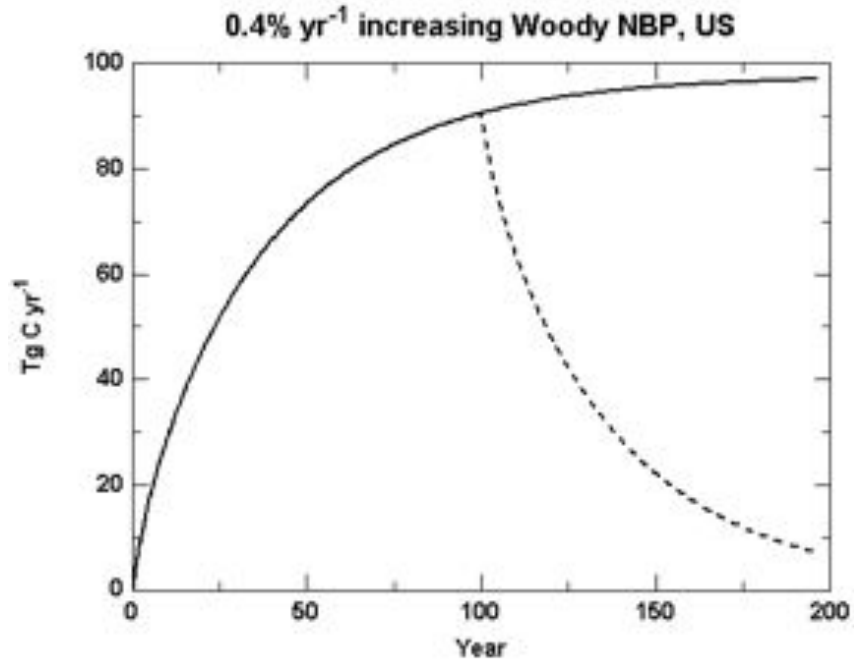
UT



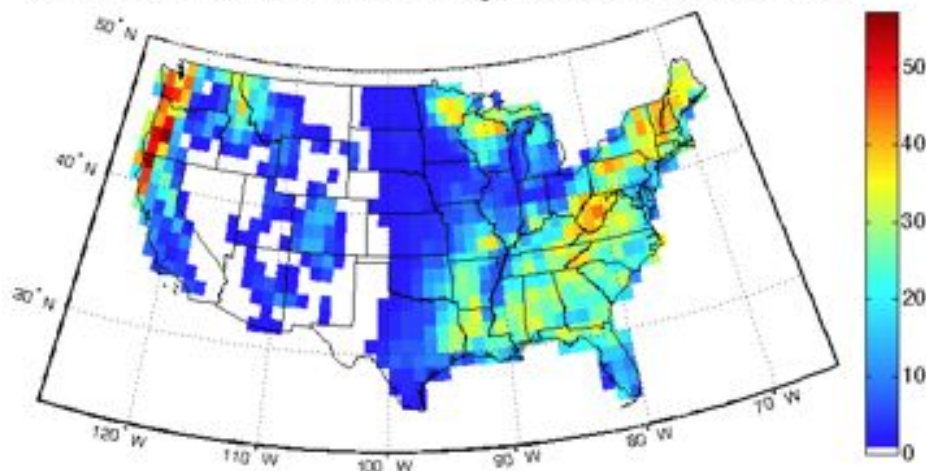
Growth Enhancement Scenario:

Increase Wood NPP at 0.4% / yr for 100 years

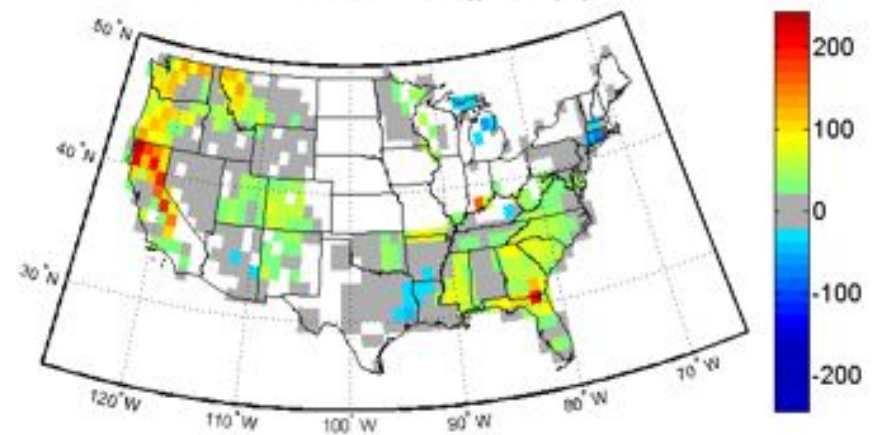
Produces a 90 Tg C / yr Sink



US NEPwood in 1850 with NPPwood increasing at 0.4% of initial NPPwood from 175



Mean Sink Enhancement [$\text{gC m}^{-2} \text{yr}^{-1}$]



Conclusions

Modeling disturbance and regrowth effects on forest NEP accounts for only half of the carbon sink seen in US stock changes

The additional sink is likely due to growth enhancements (climate trends, CO₂ fertilization, nitrogen fertilization, irrigation)

Enhancement is concentrated in regions with active management and younger and more productive forests (SE, SC, PNW, PSW)

Enhancement is supported by a number of lines of evidence.

The mechanisms driving the enhancement are unclear.

Note the Size of the enhancement exceeds expected CO₂ fertilization effects so positive feedbacks with other factors are required



Current and Future Work

- ◆ Wall-to-Wall CONUS VCT Products (PI: Goward)
- ◆ Expand spatial domain to Canada and Alaska
- ◆ Improved representation of disturbance type (fire, harvest, insect driven mortality)
- ◆ Derive finer spatial scale calibrations from FIA (state?) and account for thinning.
- ◆ Address the issue of what if anything is causing large scale growth enhancement
- ◆ Evaluate ability to detect/quantify forest source/sinks from observed atmospheric CO₂ variability (Kawa et al.)

Detecting and Quantifying Vegetation Responses to Climate Variability Using NDVI

Jim Collatz, Fanwei Zeng, Alvaro Ivanoff, Jorge Pinzon

In support of and supported by several projects (GFED, CMS, Kawa)

Rational: NDVI is used to drive the carbon cycle in diagnostic models like CASA. It is assumed that some part of NDVI variability represents real responses of vegetation to climate in these models. To do a better job at predicting interannual variability in the carbon cycle we need to understand the sources of variability in the models.

How much of the NDVI variability is caused by real climate response of the vegetation?

Data Sets:

NDVI: GIMMSg AVHRR, MODIS Terra, MODIS Aqua

Temperature: GISS and CRU

Precipitation: GPCP, TRMM

Other:

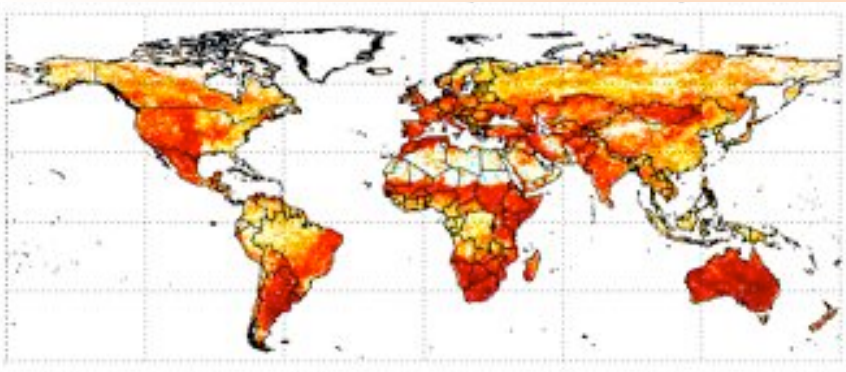
MODIS Snow Cover, MODIS Aerosol OD, MODIS Cloud Cover, GISS Solar Radiation

Weakness in AVHRR addressed by MODIS: degradation of calibration, drift, other BRDF, narrower bands (corrections for water vapor and aerosols), resolution.

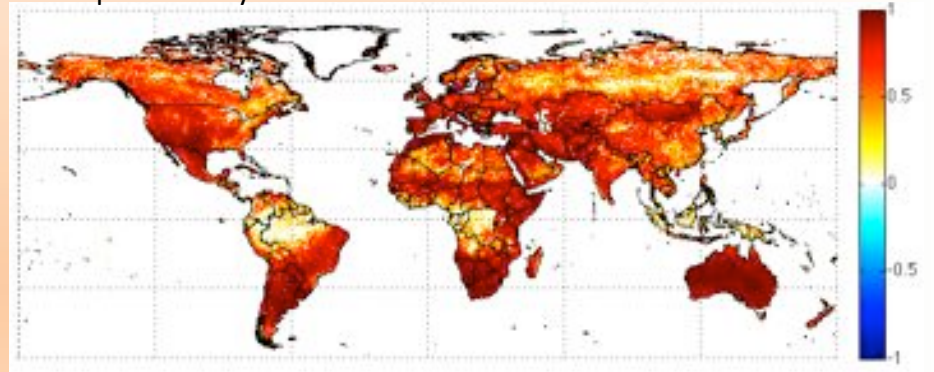
Advantages of AVHRR (esp GIMMSg): long timer period (more robust detection of climate signal), long experience with data (> 25 years)

GIMMSg NDVI captures same climate (and noise) driven variability as MODIS

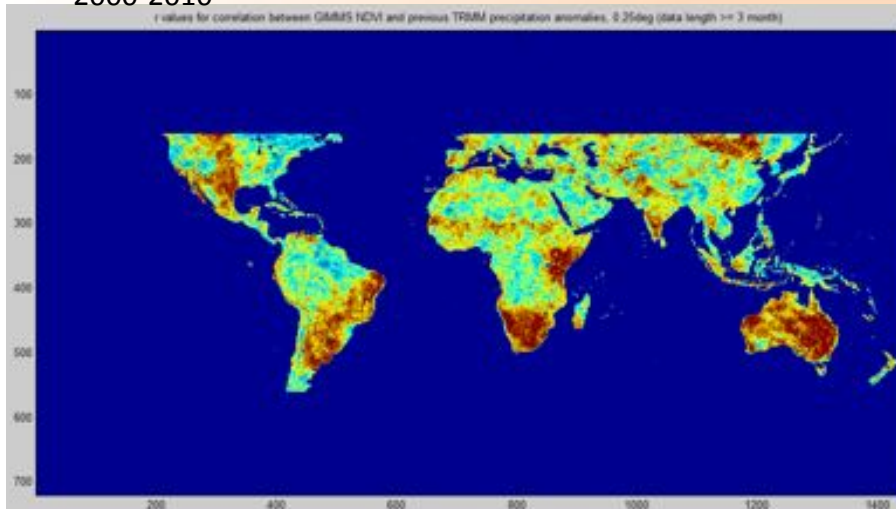
(a) Significant correlations ($p < 0.05$) between GIMMS and MODIS Aqua monthly NDVI anomalies, 2003-2010



(b) Significant correlations ($p < 0.05$) between MODIS Terra and Aqua monthly NDVI anomalies 2003-2010



Significant correlations ($p < 0.05$) between GIMMS monthly NDVI anomalies and antecedent TRMM precipitation, 2000-2010



Significant correlations ($p < 0.05$) between MODIS monthly NDVI anomalies and antecedent TRMM precipitation, 2000-2010

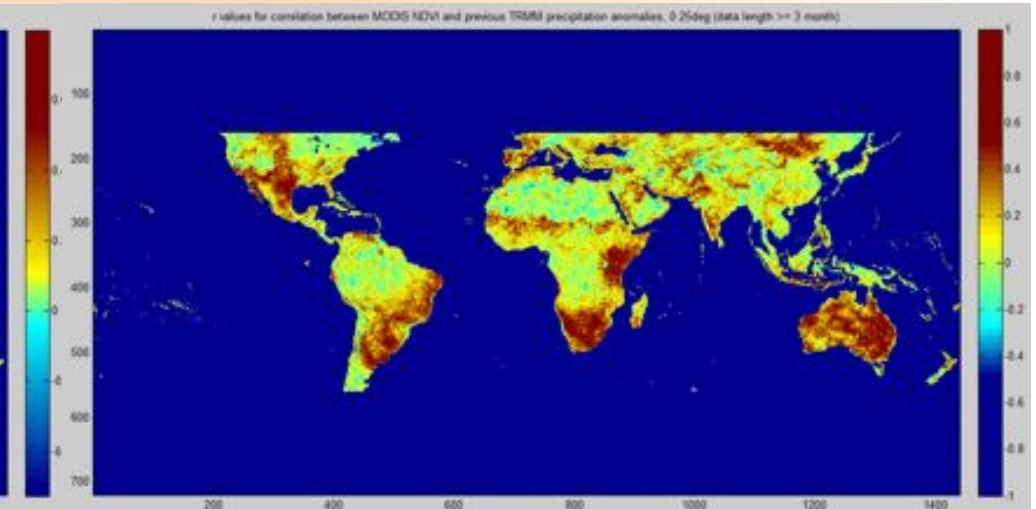


Figure 4. Global maps of month-specific correlation coefficients between GIMMS NDVI and cumulative GPCP precipitation (1-6 month lead) for 1982-2010 ($n = 29$). Only correlations significant at 95% confidence level are shown. (Spatial resolution: $1^\circ \times 1^\circ$. NH: Northern Hemisphere; SH: Southern Hemisphere)

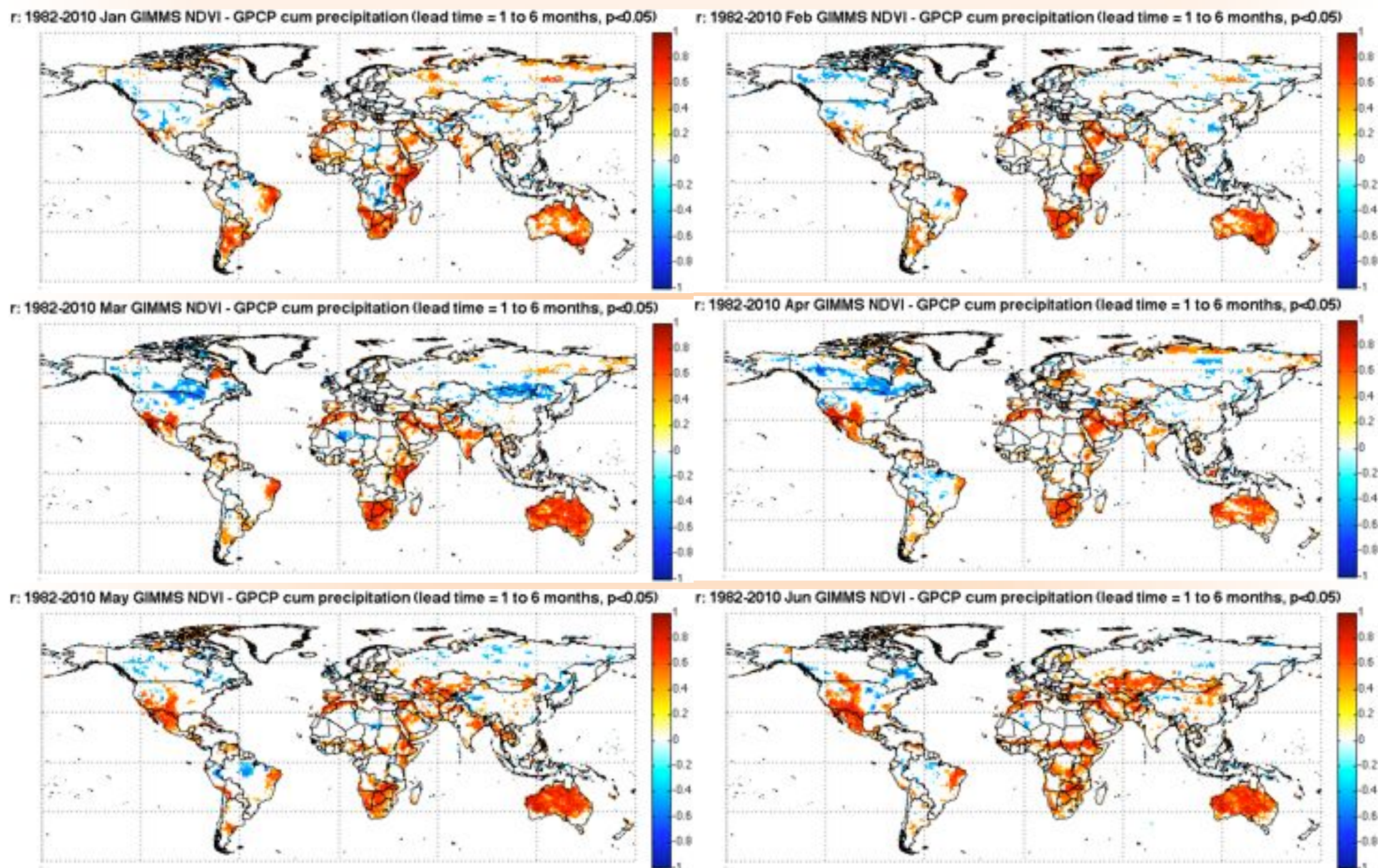
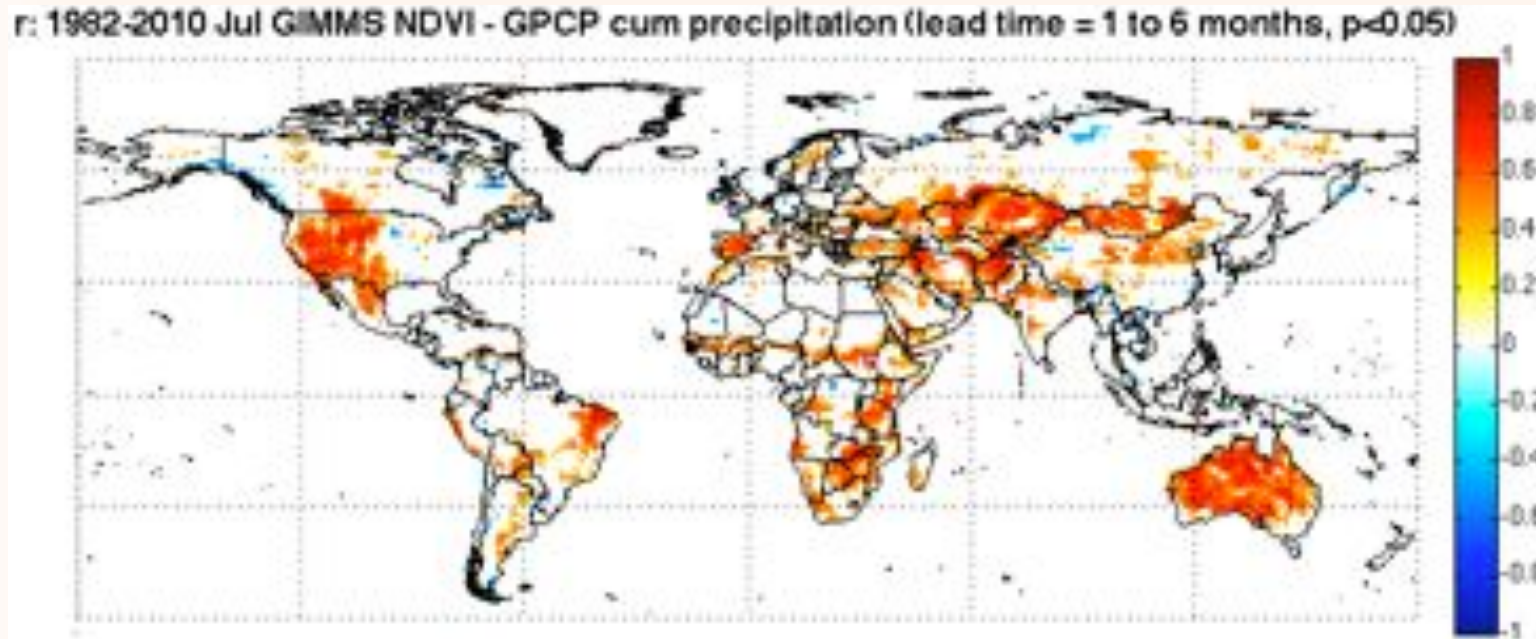
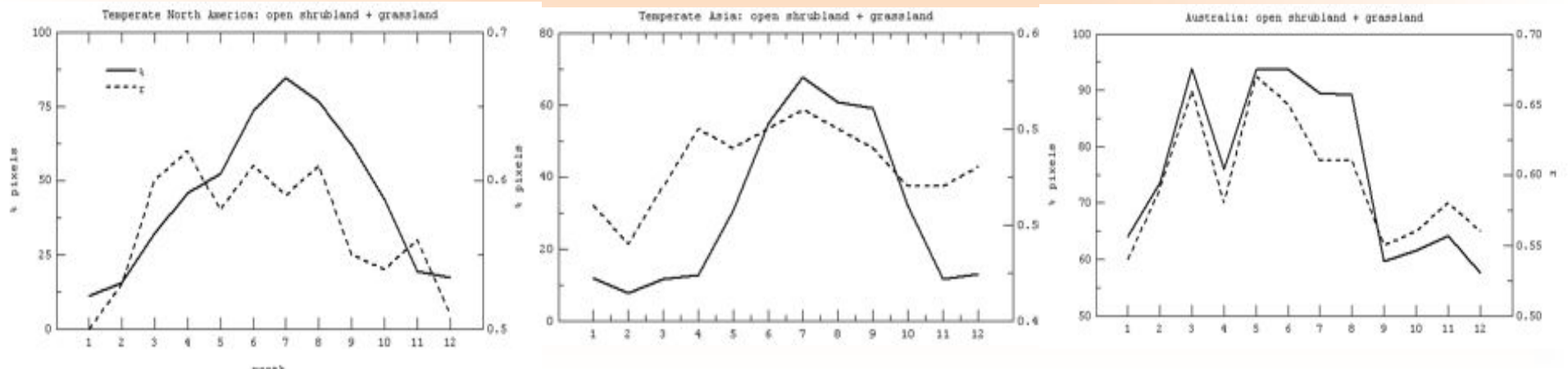


Figure 4. The correlation coefficients between GIMMS NDVI and cumulative GPCP precipitation (1-6 month lead) the month of July, 1982-2010 (n = 29). Only correlations significant at 95% confidence level are shown.



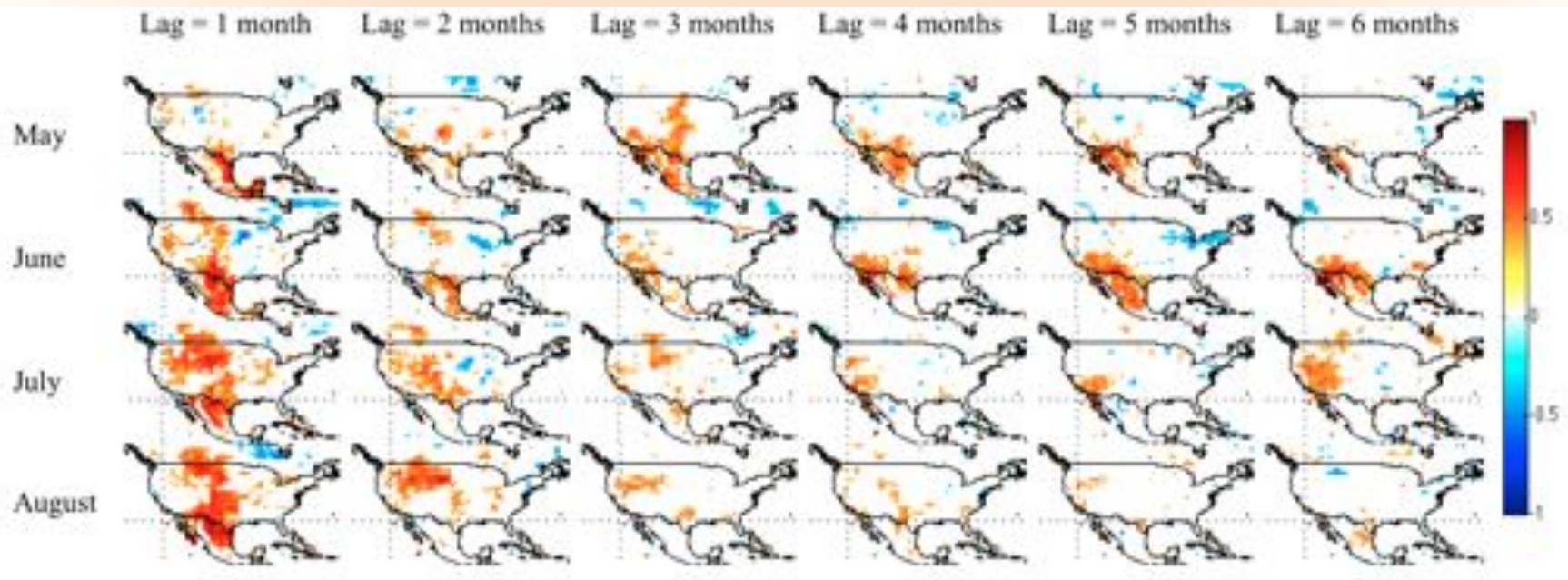
pixel % that show significant positive correlation (95% confidence level) and average correlation coefficient aggregated into certain vegetation classes and regions. Regions and classes are examples where high correlations occurred.



Correlations show that NDVI captures the seasonal dynamics of ecohydrology

Figure 5. Regional maps of month-specific GIMMS NDVI and GPCP precipitation correlations with varying lags (n = 29).

(a) North America:

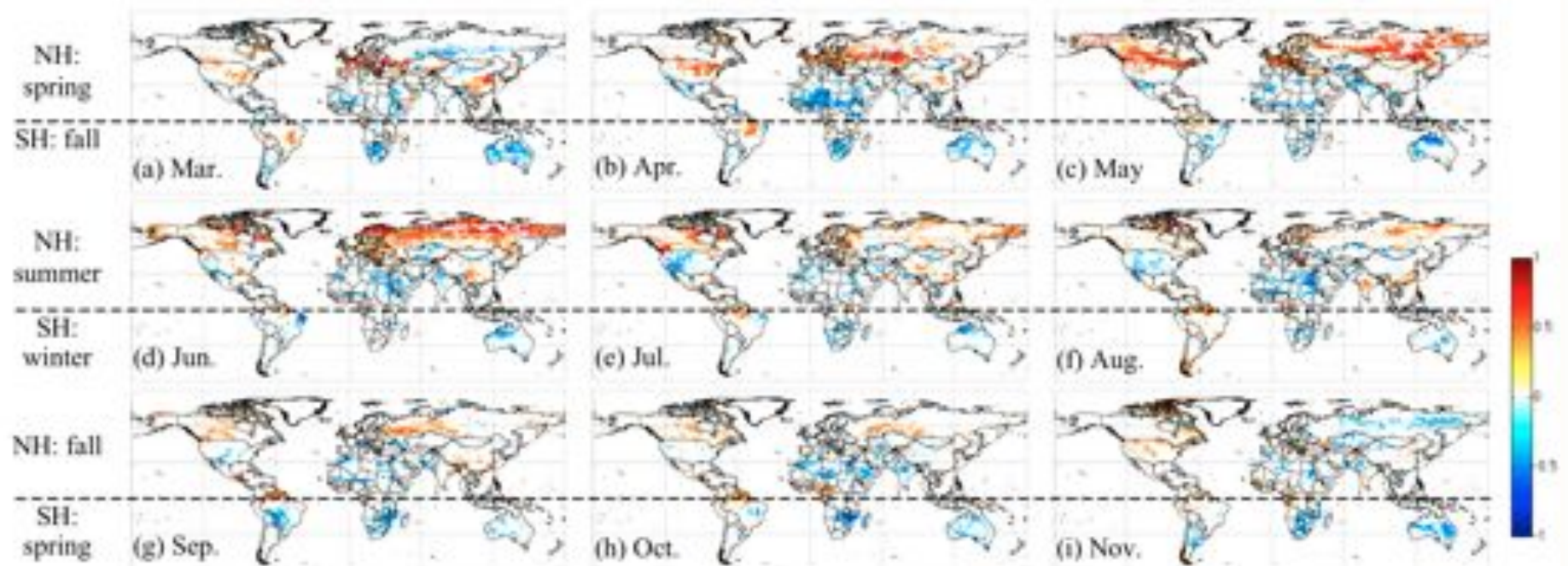


Early in the North American growing season vegetation growth is sensitive to cumulative antecedent precipitation from winter

Late in the growing season vegetation is more sensitive to recent precipitation, similar behavior in Africa and Australia.

Significant ($p < 0.05$) correlations between temperature and NDVI anomalies

Figure 7. Global maps of month-specific correlation coefficients between GIMMS NDVI and GISS temperature anomalies with lag = 0 month for 1982-2010 ($n = 29$), after removal of pixels with significant negative correlation between GIMMS NDVI and MODIS Terra snow cover. Only correlations significant at 95% confidence level are shown. (Spatial resolution: $0.5^\circ \times 0.5^\circ$, NH: Northern Hemisphere; SH: Southern Hemisphere)

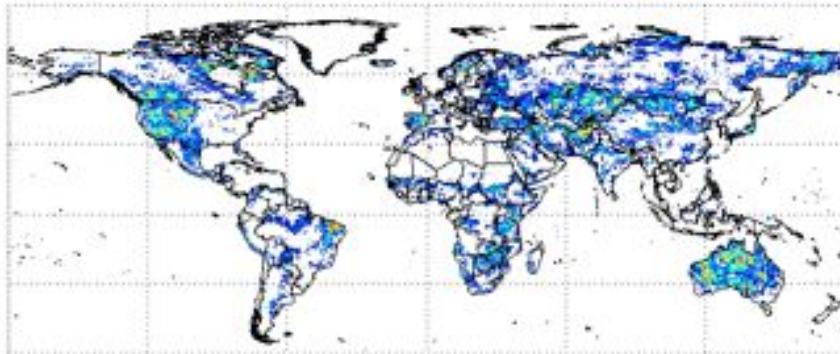


Note: negative correlations are associated with negative correlations between precipitation and temperature
-water limited conditions

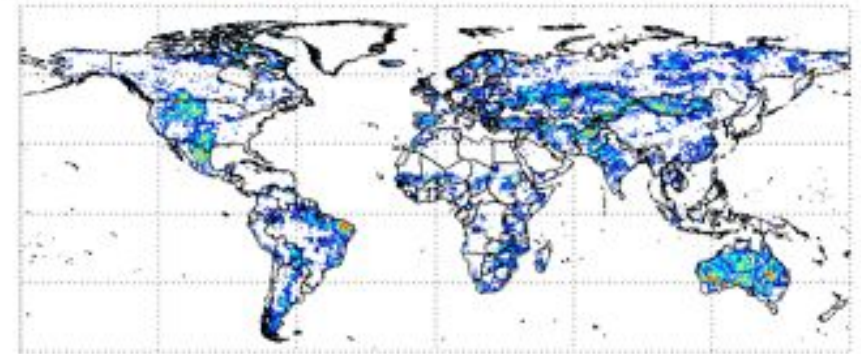
NDVI and temperature anomalies are correlated with the onset of spring in northern latitudes

The variance in NDVI explained by “real” vegetation responses to climate

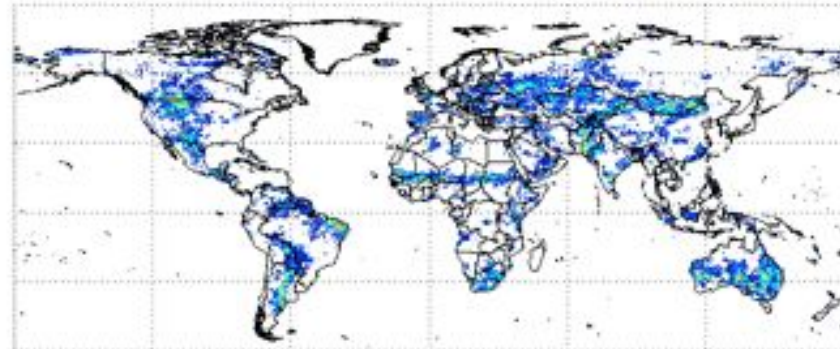
r^2 sum (82-10, Jul): positive GIMMS NDVI - cum GPCP and GISS ($p < 0.05$, no snow)



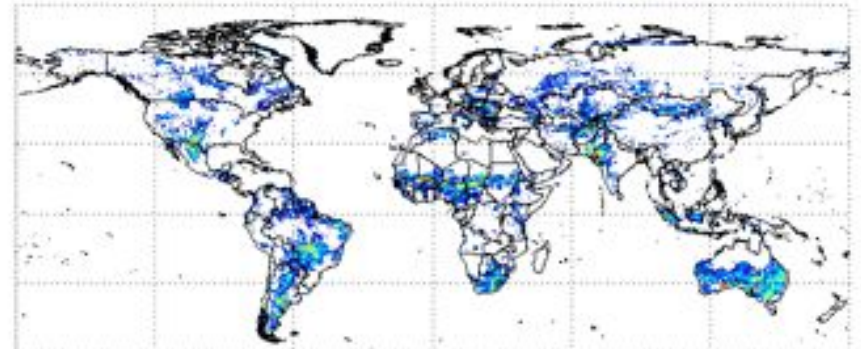
r^2 sum (82-10, Aug): positive GIMMS NDVI - cum GPCP and GISS ($p < 0.05$, no snow)



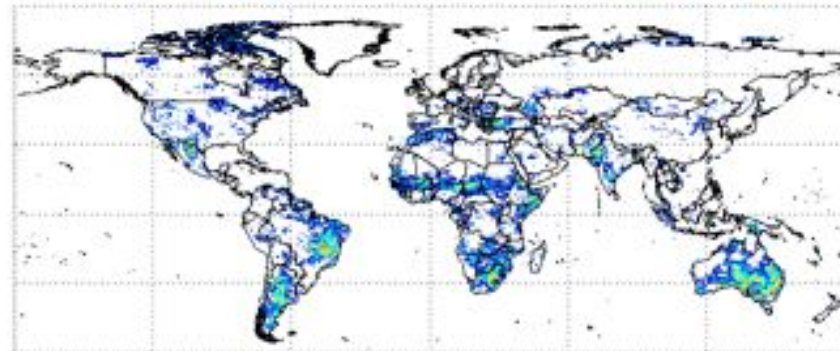
r^2 sum (82-10, Sep): positive GIMMS NDVI - cum GPCP and GISS ($p < 0.05$, no snow)



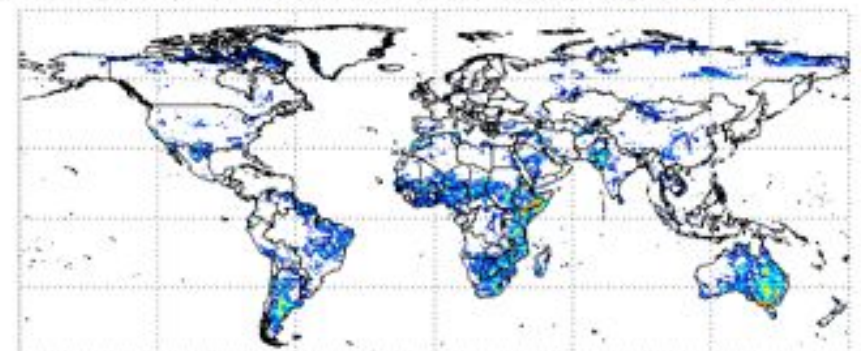
r^2 sum (82-10, Oct): positive GIMMS NDVI - cum GPCP and GISS ($p < 0.05$, no snow)



r^2 sum (82-10, Nov): positive GIMMS NDVI - cum GPCP and GISS ($p < 0.05$, no snow)



r^2 sum (82-10, Dec): positive GIMMS NDVI - cum GPCP and GISS ($p < 0.05$, no snow)

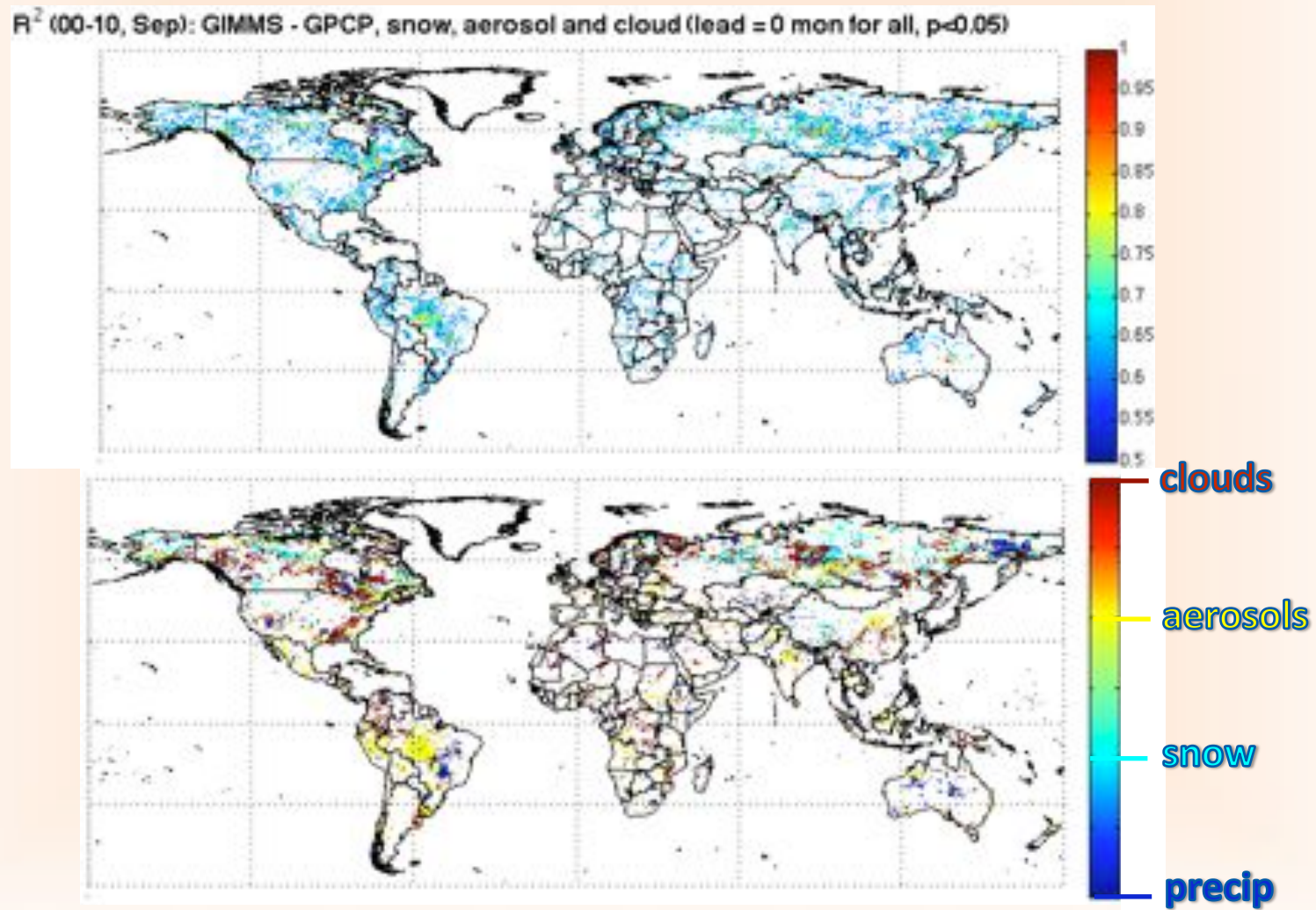


Variance in NDVI caused by noise

Variance in NDVI explained by current month precip, snow, aerosols, and clouds

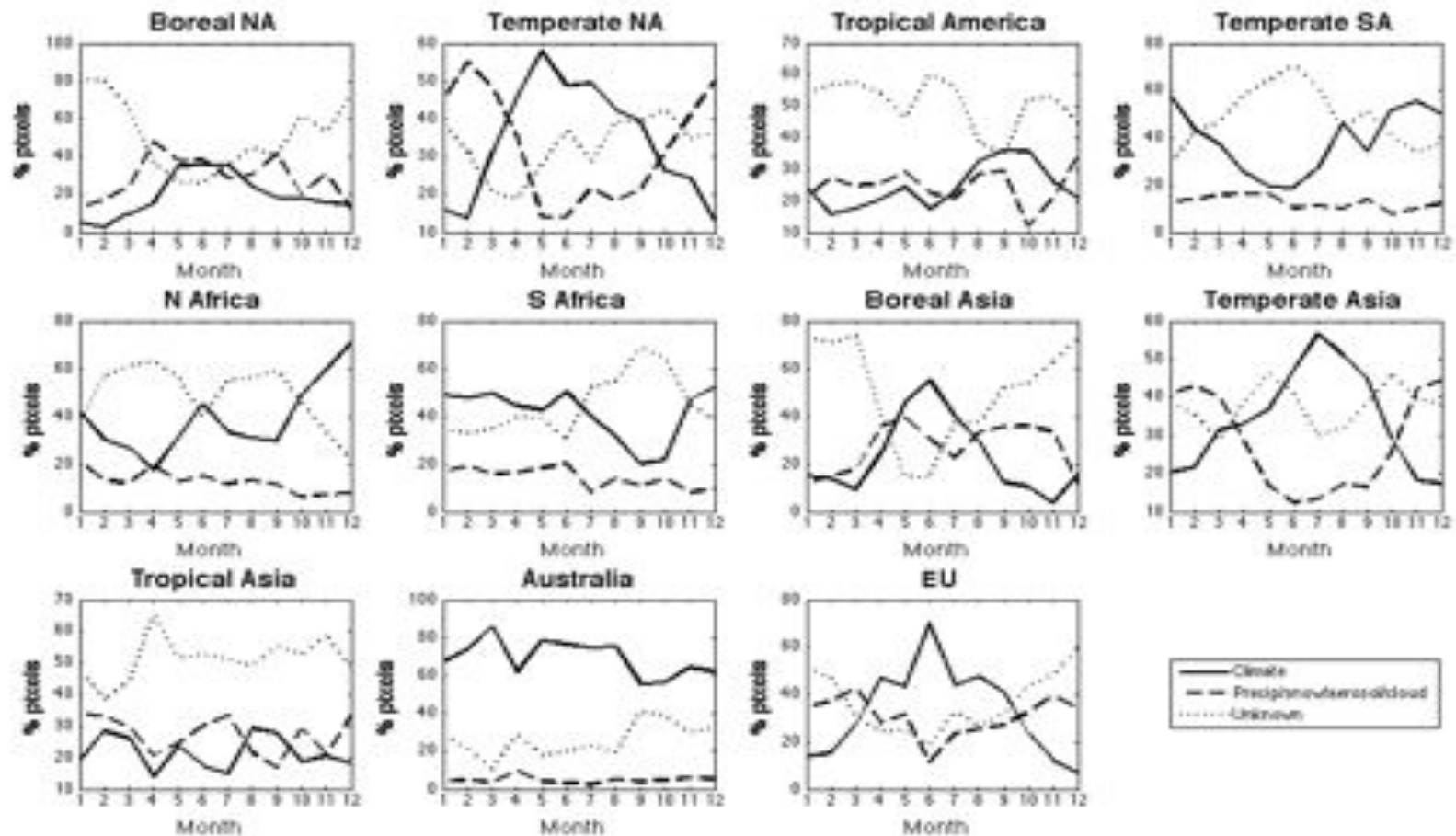
Example: September

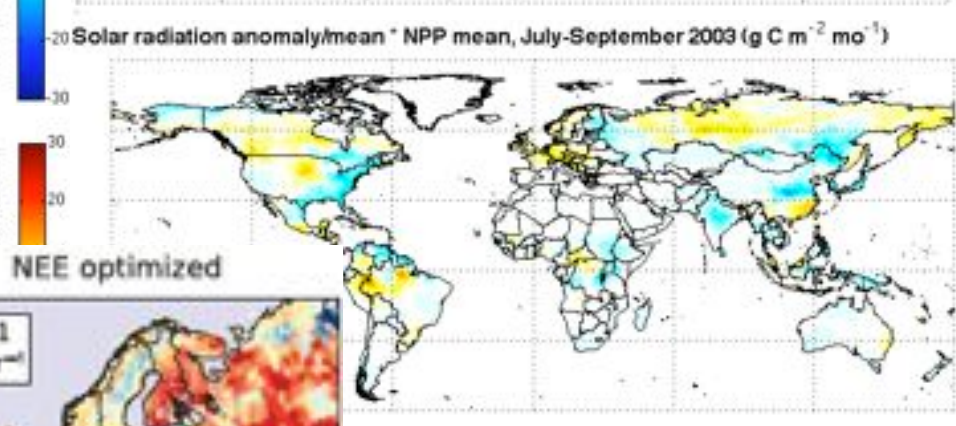
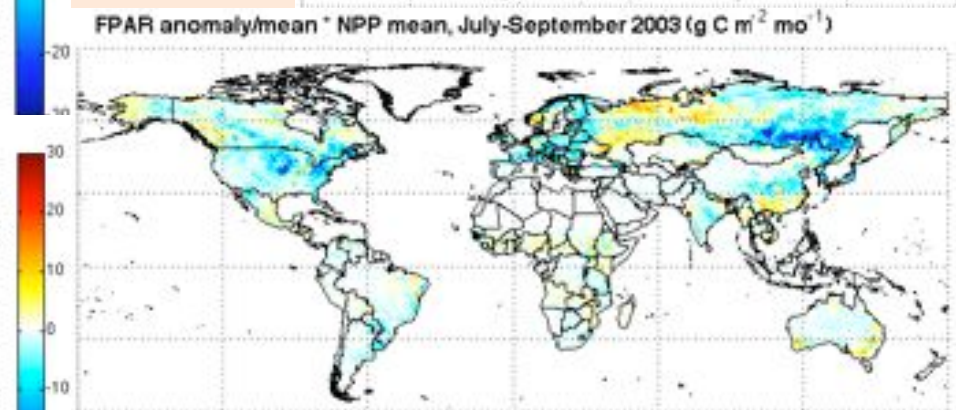
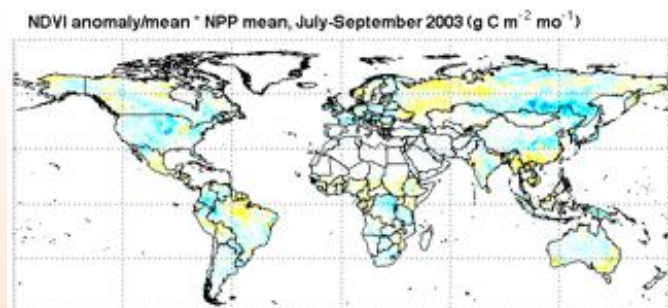
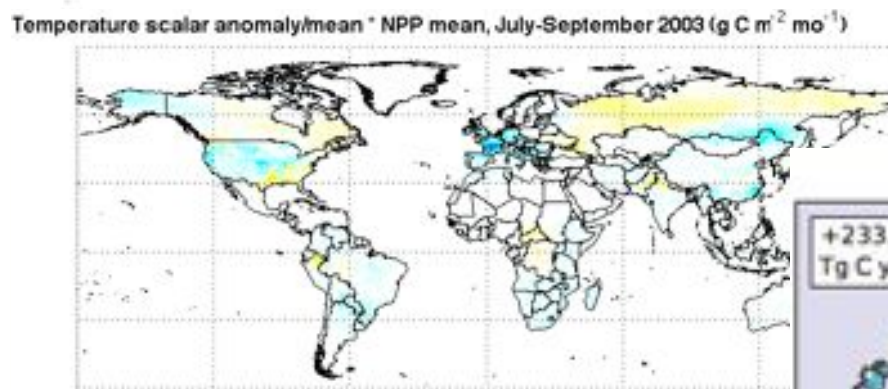
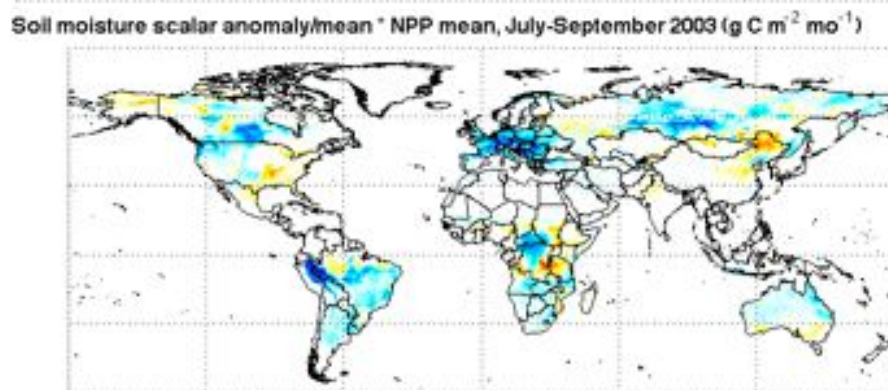
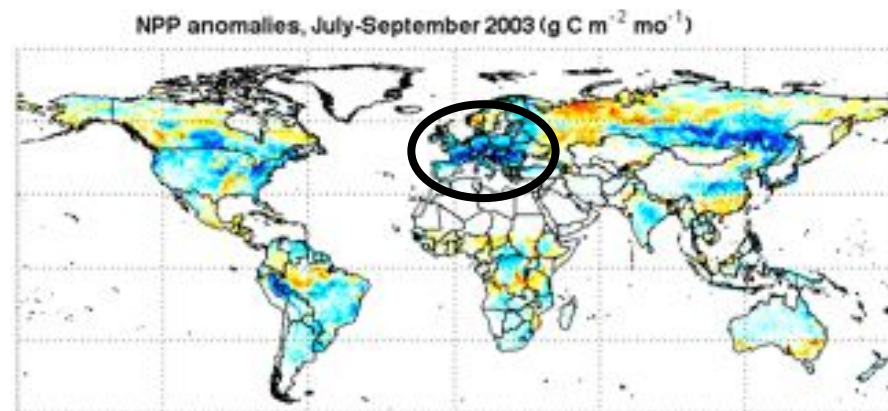
**Note all correlations are negative



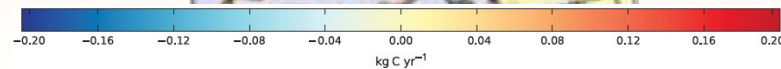
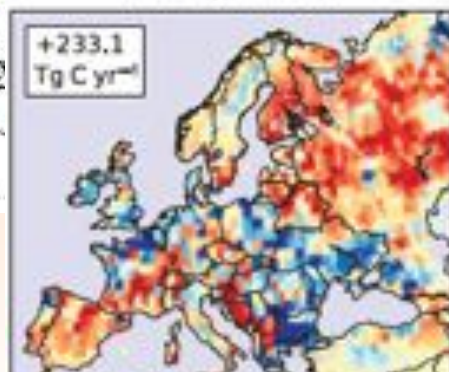
NDVI interannual monthly variance explained by:

- “real” climate responses
- - - Interference from snow, precipitation, clouds and aerosols
- Remaining unexplained causes





NEE optimized



Atmospheric CO_2 inversion
June-August 2003, Peters et al., GCB '10